Hydrogeology Journal (2018) 26:2595–2615
https://doi.org/10.1007/s10040-018-1815-1

REPORT

Tracing salinization processes in coastal aquifers using an isotopic and geochemical approach: comparative studies in western Morocco and southwest Portugal

Paula M. Carreira[1] · Mohamed Bahir[2] · Ouhamdouch Salah[2] · Paula Galego Fernandes[3] · Dina Nunes[1]

Received: 25 September 2017 / Accepted: 12 June 2018 / Published online: 29 June 2018

Abstract

Environmental stable and radioactive isotopes (δ^2H, $\delta^{13}C$, $\delta^{18}O$; ^3H and ^{14}C), together with physical and geochemical data, were used in the determination of the origins of groundwater salinization and geochemical evolution processes in coastal regions. Two case studies on the Atlantic Coast are discussed, one located in the Essaouira sedimentary basin, western Morocco, and the second, in the Lower Tagus–Sado sedimentary basin, southwest Portugal. In both regions, groundwater degradation occurs by salinization increase to different concentrations and in relation to different origins. The main quality issues for the groundwater resources are related to seawater intrusion, dissolution of diapiric structures intruding the aquifer layers, brine dissolution at depth, and/or evaporation of irrigation water. Anthropogenic pollution ascribed to agricultural activities is another source for groundwater degradation, affecting mainly the shallow aquifers. The apparent ^{14}C age of the analysed samples ranges from 2.9 ± 0.3 up to 45.6 ± 0.6 pmC in the Miocene groundwater samples from the basin in Portugal; at the Essaouira basin in Morocco, the ^{14}C content varies from 60 to 86 pmC. In most of the water samples, the ^3H concentration is below the detection limit. In both basins, the isotopic results together with the geochemical data provided an effective label for tracing the mineralization origin and groundwater degradation processes. Further, the isotopic signatures were used in the identification of a paleoclimate (colder period), recorded in the stable isotopic composition and corroborated with the ^{14}C data.

Keywords Coastal aquifers · Salinization · Groundwater age · Portugal · Morocco · MENA

This article is part of the topical collection "Coastal aquifers in the Middle East and North Africa region"

Electronic supplementary material The online version of this article (https://doi.org/10.1007/s10040-018-1815-1) contains supplementary material, which is available to authorized users.

✉ Paula M. Carreira
carreira@ctn.tecnico.ulisboa.pt

Mohamed Bahir
bahir@uca.ma

Paula Galego Fernandes
ppfernandes@ciencias.ulisboa.pt

[1] Centro de Ciências e Tecnologias Nucleares (C2TN), Instituto Superior Técnico, Universidade de Lisboa, Estrada Nacional N° 10, ao km 139,7, 2695-066 Bobadela LRS, Portugal

[2] Ecole Normale Supérieure, Cadi Ayyad University, Marrakesh, Morocco

[3] Instituto D. Luiz, Campus Universitário, Campo Grande, Lisboa, Portugal

Introduction

Groundwater systems constitute an important and sometimes unique source of drinking water supply in many parts of the world. Freshwater availability is under increasing pressures connected to human activities, varying from water abstraction to contaminating activities such as agriculture and livestock production, which threaten drinking water resources and irrigation supplies. Other than these possible sources of contamination, in coastal regions, the groundwater resource is often vulnerable to seawater intrusion and to polluted-water seepage from upper unconfined aquifers. Day by day, demand for good quality water is rapidly increasing, leading to processes of salinization that threaten the exploitation of additional water resources. Salinization can be the result of processes related to both seawater intrusion and water–rock interaction mechanisms, among them, adsorption of Na by the aquifer matrix, with release of Ca, which is a process that is activated when seawater intrusion occur (Shi et al. 2001; Custodio 2002; Pulido-Leboeuf 2004; Jalali 2007; Bouchaou et al. 2008;

Mondal et al. 2011; Ben Hamouda et al. 2013). Besides this, contributing to the increase in pressure on water resources, the expansion of agricultural areas and the excessive use of fertilizers are responsible for another source of groundwater salinization (Kim et al. 2003). The relation between human activities and the increase of salinization of groundwater resources is well documented for situations whereby freshwater is reused in agricultural activities. In this case, the increase of salinization is not only associated with the introduction of fertilizer and pesticides, but also associated with open irrigation channels, which are easily subject to water evaporation and will lead to an accumulation of salts in the remaining fraction. In addition, irrigation return flows can alter natural groundwater salinity.

Knowledge of groundwater flow in an aquifer system is an important tool in the development of a conceptual circulation model. Such a model must consider the geological layers (water–rock interaction processes) and the transport of dissolved salts. In the case of sedimentary basins, models should account for the presence of salt structures or minerals dispersed within the basin layers, as the flow model will be sensitive to these features. In these specific types of investigation, the isotope hydrology approach can provide additional information concerning the groundwater systems (Carreira et al. 1996, 2014); the isotope data will serve as a sometimes crucial tool in identifying the salt origins (Pulido-Leboeuf 2004; Bahir et al. 2008; Galego Fernandes et al. 2009; Stadler et al. 2012; Carreira et al. 2014).

The origin of groundwater salinization in coastal regions has been investigated using a variety of different approaches, from physical-geochemical data to environmental isotopes, and via the traditional hydrogeological tools to statistical approaches. For example, Bouzourra et al. (2015), in the shallow coastal aquifers of Aousja-Ghar El Melh and Kalâat el Andalous, NE Tunisia, identified the origin and processes of groundwater salinization through geochemical and statistical approaches (using principal components analysis, PCA), while Re et al. (2013) identified and characterized the main processes causing groundwater salinization in the coastal aquifer of Bou-Areg (Morocco) by a multi-tracer geochemical approach (chemical data and environmental isotopes).

As mentioned by Custodio (2010), not only the semiarid regions in African and Mediterranean countries are facing degradation/mineralization of groundwater coastal resources; Europe is also handling an increase in aquifer salinization ascribed to the long coastline in which human activities are concentrated. Salinization problems have been growing with more intensive groundwater abstraction from a range of geological formations—for example deltaic areas (Rhine-Meuse in The Netherlands; Aveiro in N Portugal; Llobregat in northeastern Spain), in the detritical coastal formations of Belgium and northern France, and in the carbonate coastal massifs in Italy. In addition, a growing concern for the southwestern USA aquifers has been reported by Langman and Ellis (2010), as depletion of freshwater aquifers is linked with the potentiometric-surface relationship with deeper aquifers, which can induce saltwater intrusion due to the increase of hydraulic gradient. In Australia, freshwater-resource salinization by seawater intrusion has been reported in several regions, from Queensland to Western and Southern Australia, ascribed to extended periods of low rainfall and abstraction increase, associated with a population increase along the coast (Werner 2010).

One of the main goals of this hydrogeological study is the identification of the key mechanisms responsible for groundwater degradation triggered by an increase in mineralization. Use of the isotopic composition (tritium and carbon-14) and its relation with geochemical parameters, can provide an effective label/tool in the identification of the main cause of this problem (seawater–groundwater mixing; active seawater intrusion vs. ancient seawater; dissolution of salt domes or dissolution of minerals dispersed in the geological layers, for example).

Natural processes of water–rock interaction are the main mechanisms responsible for water mineralization within the two research areas chosen, although this trend can be locally disturbed by anthropogenic activity in agricultural areas by the addition of fertilizer or even due to salts concentration by evaporation of irrigation water. The two research areas are on the Atlantic Coast: the Essaouira basin in western Morocco, and the Lower Tagus-Sado basin in southwest Portugal. Both research areas are located in sedimentary basins, and cation exchange processes can easily occur with the uptake of Na dissolved in the groundwater and release of Ca by the aquifer matrix, leading to an increase in groundwater mineralization.

The main goal of this report is to investigate and compare the origins and variation of solutes present in the two similar sedimentary coastal aquifers, using the same methodologies. The same analytical tools (environmental isotopes and geochemical data) were used in a similar geological and climatic context, and different conclusions can be obtained concerning the origin of salinization and degradation of both groundwater resources. The combination of isotopic data and geochemical data interpretation in a hydrogeological context will be presented and discussed, bearing in mind that the main objective is the identification of the key mechanisms responsible for groundwater degradation in both regions.

A secondary objective of this study is to understand the relation of these coastal systems (discharging directly to the sea) to sea-level fluctuations under a climatic-change scenario that will affect directly the system dynamics. These aquifers can represent potential archives of past climatic events, since the changes in the isotopic composition of the oceans during a glaciation period can be recorded in the paleowaters. The paleoclimate evidences encoded in groundwater composition

(isotopic signatures) will allow the extraction of information and help in the reconstruction of past environments (Plummer 1993; Carreira et al. 1996; Carreira 1998; Edmunds and Droubi 1998; Galego Fernandes and Carreira 2008; Re and Zuppi 2011; Foster and MacDonald 2014).

Study areas: geological and hydrogeological settings

Essaouira basin (Morocco)

The first research area is located in Morocco on the Atlantic Ocean coast, in the upper zone of the Essaouira sedimentary basin, in the vicinity of Essaouira municipality (Fig. 1). The area is delimited by the Atlantic Ocean to the west, Mramer Wadi basin to the N and NE, and by Igrounzar Wadi crystalline massive in the E and SE.

From the geological point of view, sedimentary layers from the Triassic to Quaternary fill Essaouira basin, covering a Palaeozoic basement. The Triassic deposits crop out in the eastern and southern parts of the region (Fig. 1), and marly sediments of Lower Cretaceous to Cenomanian overlie the Jurassic layers composed by carbonate rocks. Duffaud et al. (1966) in Galego Fernandes et al. (2009) call attention to the presence of Senonian gypsy marls covered by the Plio-Quaternary detrital deposits of sands, conglomerates and sandstones. The geological structures delineate a syncline bordered by the Tidzi diapir, of Triassic age, outcropping east and south. The main deformations within Essaouira sedimentary basin are represented by circular diapirs such as the Kechoula structure, NE–SW to WNW–ESE trending folds, and by strike-slip faults and by fault zones injected or not by Triassic salt, trending NNW–SSE to ENE–WSW (Medina 1989; Broughton and Trepanier 1993; Mehdi 1994 in Galego Fernandes et al. 2009).

Under the influence of the Atlantic Ocean and continental processes, Essaouira region is characterized by a cool dry season (January mean temperature around 10 °C) followed by a hot dry season (26–27 °C, July average temperature), reflected through large spatial and temporal precipitation variability. The mean annual rainfall ranges from 400 to 560 mm in the High Atlas to approximately 280 mm in the plains (Bahir et al. 2008, 2015).

Two main aquifer systems have been identified in the region: (1) a multi-layer aquifer mainly composed by detritial deposits (sandstones, conglomerates and sands) of the Mio-Plio-Quaternary age, responsible for the majority of water supply to the population. This contacts directly with the Triassic and Cretaceous formations beneath; and (2) calco-dolomitic layers of Cenomanian-Turonian age (Bahir et al. 2015), representing a karstic aquifer, according to Rachid et al. (2014), the Turonian horizon crops out on the Jbel Kchoula between 400 and 700 m above sea level (a.s.l.), while the Plio-Quaternary layers crop out between the sea level and 300 m a.s.l. The Essaouira basin is represented by a succession of syncline and anticline structures, crossed by deep fault systems, ascribed to the Atlas tectonic and Triassic diapirs formation (Rachid et al. 2014).

Lower Tagus–Lower Sado Basin (Portugal)

The second studied region is located south of Lisbon, part of the Lower Tagus–Lower Sado sedimentary basin. The Miocene aquifer constitutes an important water resource for a large highly industrialized region with highly populated urban areas. The mean annual temperature in the region is around 16 °C, and the mean annual precipitation ranges between 500 and 700 mm. About 15% of the precipitation contributes to the annual recharge.

From the geological and structural point of view, the Lower Tagus–Lower Sado basin is characterized by a huge synclinal structure composed by Tertiary sediments, mainly formed by marine deposits (Simões 2003). Alluvial and fluvial terraces are made out of sands and clays representing the Quaternary and the Pliocene layers, overlaying the Miocene deposits composed by sandstones and limestones of marine origin related to different marine transgression and regression events (Fig. 2). These deposits together show an average thickness around 200 to 300 m, although in the central part of the basin these values increase up to 800 m (Simões 2003). Geophysical studies performed by Astier (1979) in the region indicate the presence of a graben structure at a depth to which a "saline formation" was identified. Geological and geophysical data are not in agreement with the type of saline structure associated with Setúbal-Pinhal Novo graben; a brine formation unit, ancient seawater trapped in the sediments, or a diapiric structure at depth are the main hypotheses formulated to explain the increase in the groundwater mineralization.

Three main groundwater systems are recognized in Sado basin: (1) the shallow Quaternary aquifer constituted by the alluvial formations; (2) the Pliocene fluvial terraces composed by the sands and clay layers; and (3) the Miocene deposits made of sandstones and limestones, representing the main water resource in the region (Simões 2003).

Materials and methods

Sampling and analytical approach

With the main goal of combining isotopic and geochemical data to trace and compare the salinization origin of the two sedimentary basins, the selected methodological approach was similar for both studied basins. In Essaouira basin, two field campaigns were carried out, during 2004 and 2006; 20 water samples from springs, dug wells and boreholes, from the coast to inland, were collected and analysed. Physico-

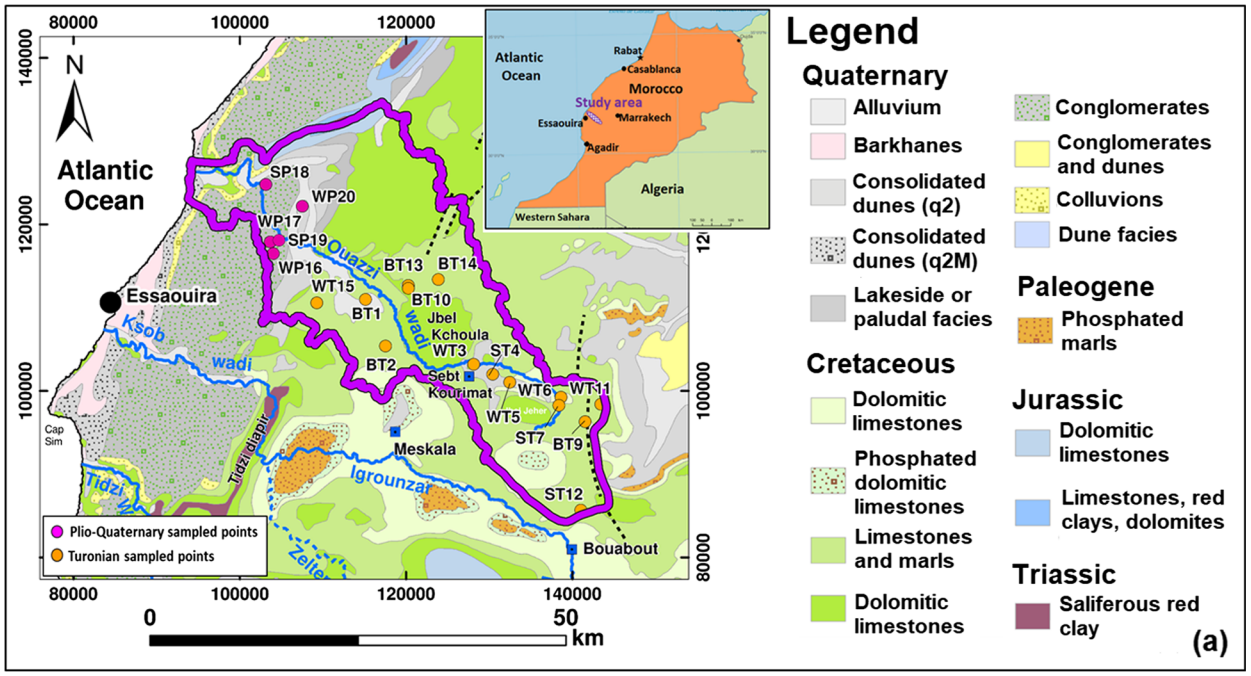
80000
100000
120000
140000
N
Atlantic Ocean
SP18
WP20
WP17
SP19
WP16
WT15
BT13
BT14
BT10
BT1
Jbel Kchoula
WT3
ST4
BT2
Sebt
Kourimat
WT6
WT11
WT5
ST7
BT9
ST12
Essaouira
Ksob wadi
Quazzi wadi
Cap Sim
Tidzi
Tidzi diapir
Meskala
Igrounzar
Zelten
Bouabout
Plio-Quaternary sampled points
Turonian sampled points
0
50
km
Atlantic Ocean
Rabat
Casablanca
Morocco
Study area
Essaouira
Marrakech
Agadir
Algeria
Western Sahara
Legend
Quaternary
Alluvium
Barkhanes
Consolidated dunes (q2)
Consolidated dunes (q2M)
Lakeside or paludal facies
Conglomerates
Conglomerates and dunes
Colluvions
Dune facies
Paleogene
Phosphated marls
Cretaceous
Dolomitic limestones
Phosphated dolomitic limestones
Limestones and marls
Dolomitic limestones
Jurassic
Dolomitic limestones
Limestones, red clays, dolomites
Triassic
Saliferous red clay
(a)

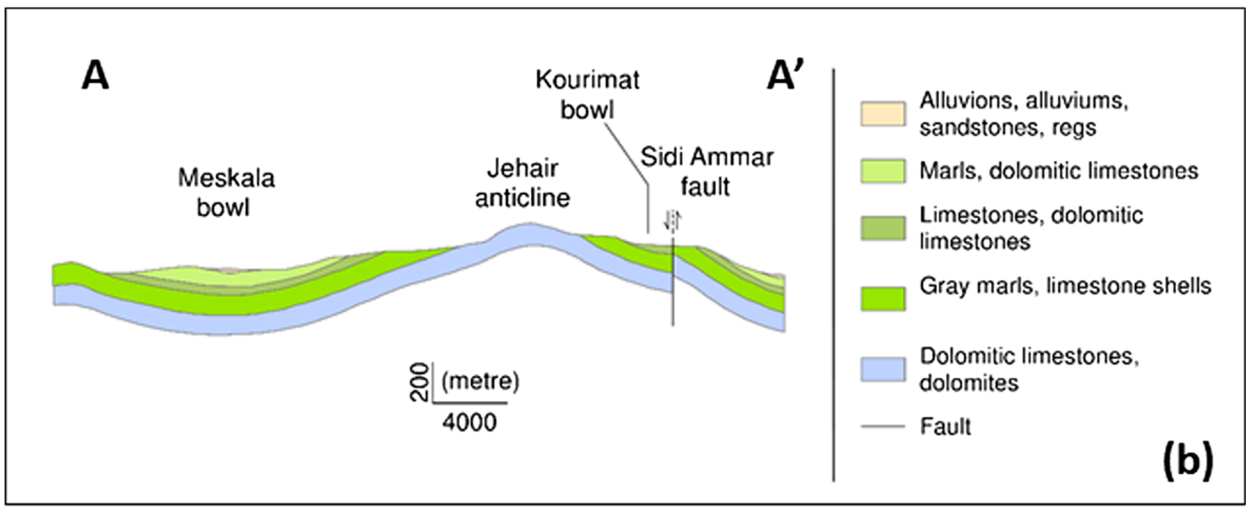
A
A'
Kourimat bowl
Sidi Ammar fault
Meskala bowl
Jehair anticline
200
(metre)
4000
Alluvions, alluviums, sandstones, regs
Marls, dolomitic limestones
Limestones, dolomitic limestones
Gray marls, limestone shells
Dolomitic limestones, dolomites
Fault
(b)

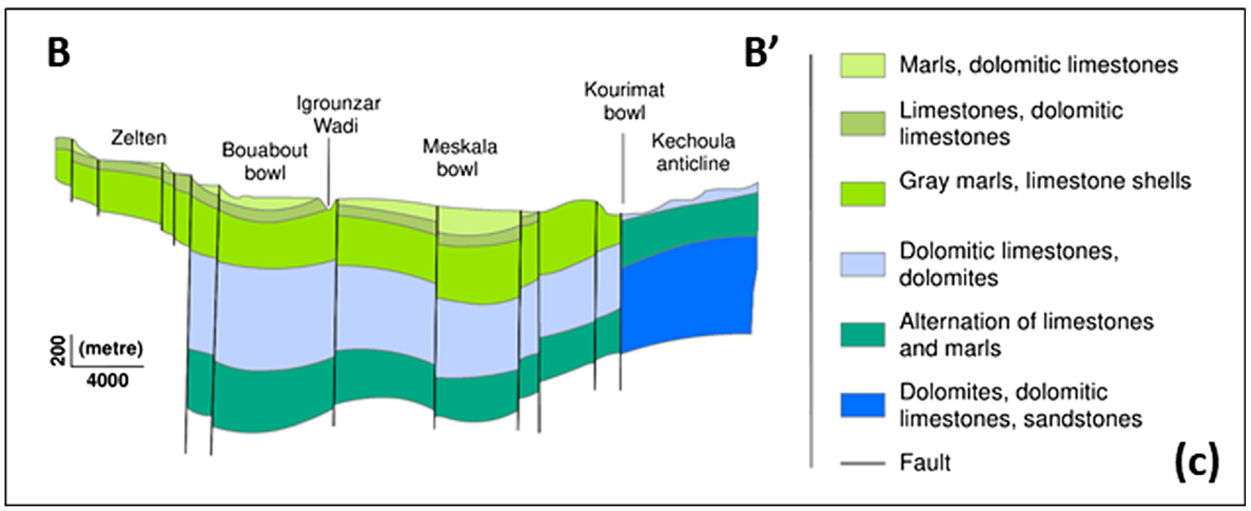
B
B'
Zelten
Bouabout bowl
Igrounzar Wadi
Meskala bowl
Kourimat bowl
Kechoula anticline
200
(metre)
4000
Marls, dolomitic limestones
Limestones, dolomitic limestones
Gray marls, limestone shells
Dolomitic limestones, dolomites
Alternation of limestones and marls
Dolomites, dolomitic limestones, sandstones
Fault
(c)

◀ **Fig. 1** **a** Essauoira regional map with the groundwater sample locations (W Morocco). The orange circles represent the sampled Turonian aquifer points; the pink circles represent the Plio-Quaternary sampled points. **b**–**c** Schematic cross sections of Essaouira sedimentary basin

chemical parameters such as temperature, pH, and electrical conductivity were determined in situ. Total alkalinity was measured a few hours after collection in the laboratory. The chemical analyses (major anions and cations) were performed at the GEOLAB Laboratory University of Marrakech (Morocco) using the following methods: atomic absorption spectrometry for Ca^{2+} and Mg^{2+}; emission spectrometry for Na^{+}, K^{+}; ion chromatography for SO_4^{2-}, NO_3^{-} and Cl^{-}. The isotopic composition was determined by the IAEA-IHS (International Atomic Energy Agency-Isotope Hydrology Section) laboratories in Vienna, Austria. The δ^2H and $\delta^{18}O$ composition was obtained by mass spectrometry; the ^3H concentration was obtained using the electrolytic enrichment

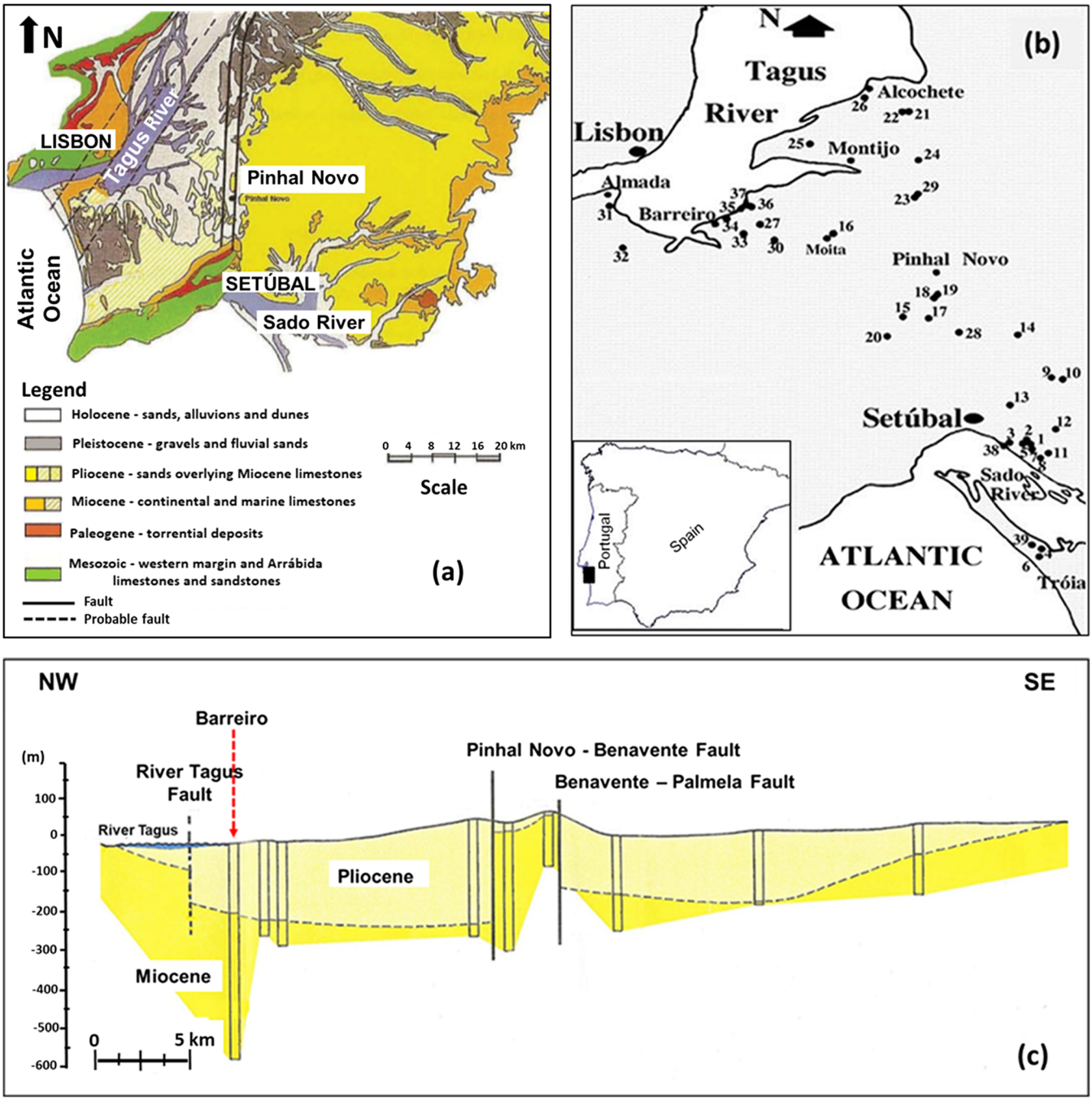

Fig. 2 **a** Lower Tagus–Lower Sado basin geology and tectonics (adapted from Simões 2003); **b** Location of the sampling sites; **c** Schematic cross section of the Lower Tagus–Lower Sado basin (adapted from Simões 1998 and from Carreira et al. 2014)

followed by the liquid scintillation counting method (IAEA, 1976). The ^{13}C and ^{14}C determinations were carried out on the total dissolved inorganic carbon (TDIC) of the groundwater, precipitated in the field as $BaCO_3$ at a pH higher than 9.0 and afterwards measured by liquid scintillation counter. The $\delta^{13}C$ values were obtained by mass spectrometry.

In the Lower Tagus–Lower Sado basin, 40 boreholes were selected and sampled in five fieldwork campaigns between November 1996 and 1999, tapping both the shallow (Pliocene) and the deep confined aquifer (Miocene). The following determinations were performed:

1. The major cations and anions were measured in the Portuguese National Water Authority laboratories using the following methods: atomic absorption for Ca^{2+} and Mg^{2+}; emission spectrometry for Na^+ and K^+; and ion chromatography for SO_4^{2-}, NO_3^- and Cl^-. The total alkalinity was measured a few hours after collection.
2. All the isotopic determinations were performed at C^{2}TN/IST (Portugal) laboratories, using the mass spectrometer SIRA 10 VG-ISOGAS for δ^2H, $\delta^{13}C$ and $\delta^{18}O$ determinations. The ^3H concentration in the water samples was obtained using the electrolytic enrichment followed by the liquid scintillation counting method (PACKARD Tri-Car-Carb 2000 CA/LL), and the radiocarbon determinations were carried out in TDIC, precipitated in the field as $BaCO_3$ at a pH environment higher than 9.0. In the laboratory, the barium carbonate was transformed into benzene using a synthesis line and afterwards measured by a liquid scintillation counter (PACKARD Tri-Carb 2770 TR/SL).

The groundwater isotopic composition ($^2H/^1H$ and $^{18}O/^{16}O$ ratios) are reported versus the V-SMOW standard, using the conventional δ-notation, whereas $^{13}C/^{12}C$ ratios of dissolved inorganic carbon are reported versus V-PDB (Coplen et al. 1996). The overall precision was better than ±1 ‰ for δ^2H and ± 0.1 ‰ for $\delta^{18}O$, following the analytical methods of Friedman (1953) and Epstein and Mayeda (1953). In the case of $\delta^{13}C$, the overall precision was around ±0.1‰. The ^3H concentration was determined by liquid scintillation counting after electrolytic enrichment. The error associated with the ^3H measurements (usually around 0.6 TU (tritium units) varies with the ^3H concentration in the sample. ^{14}C concentration is expressed in pmC (percentage modern Carbon). The errors associated with this method vary with the concentration of carbon available in each sample, and increase with the decrease of the ^{14}C concentration in the sample (IAEA 2014). For both regions, tritium analyses were carried out for all sampled water points; however, in a selection of samples, radiocarbon determinations were also performed, depending on the accessibility of the points and the available budget.

Data treatment

Geochemical calculations

The chemical data were represented in a Durov diagram in order to evaluate the groundwater chemical evolution along the flow paths and relation/pattern within the water samples. The program HIDSPEC, a hydrogeochemical model that calculates the speciation of natural waters (Carvalho and Almeida 1989), was used to calculate the saturation indexes (SI) of all the groundwater samples collected in the two research areas. Based on the geological layer, the saturation indexes chosen were with respect to calcite, dolomite, gypsum and halite. The same program was also applied to estimate the ionic balance for each water sample.

Moreover, ionic exchange between the clay matrix and the groundwater has a very important role in the geochemical evolution and facies of the water systems, in particular in sedimentary basins, like in Essaouira and the Lower Tagus-Lower Sado basins. The ion exchange "process" is able to modify the ion concentration in the aqueous system to a varying degree. In order to investigate the importance of this process, ion exchange for Ca^{2+} and Na^+ was calculated by comparing the difference (Δn) of the measured concentration ($n_{(m)}$) and that expected if mixing with seawater is occurring ($n_{(c)}$). This Eq. (1) proposed by Pennisi et al. (2006) is based on the Cl^- concentration (conservative ion) and the "mobility behaviour" of Na and Ca:

$$\begin{aligned} \Delta n_X &= n_{X(m)} - n_{X(c)} \\ \Delta n_X &= n_{X(m)} - \left[n_{X(0)} + \left(n_{Cl(m)} - n_{Cl(0)} \right) \left(n_{X(sea)} / n_{Cl(sea)} \right) \right] \end{aligned} \quad (1)$$

where $n_{X(0)}$ and $n_{Cl(0)}$ are the concentrations of ions X and Cl^- in groundwater not affected by sea water intrusion (mean composition).

Stable isotopes (δ^2H and $\delta^{18}O$)

The groundwater recharge (in both areas) is derived from direct infiltration of precipitation; groundwater samples in this case will reflect the mean isotopic composition of that regional precipitation. Sometimes a difference is observed between the groundwater isotopic composition and the composition of the regional precipitation. In this situation, assuming that a deviation occurs between the groundwater and the regional precipitation, an explanation for this variation must be sought (Fig. 3). Two different hypotheses can be formulated on the assumption that no evaporation before infiltration has occurred and no mixture between different aquifer units is happening: (1) recharge can be derived from a different source other than regional precipitation, for example surface water (rivers, lakes or dams); (2) precipitation recharge has occurred

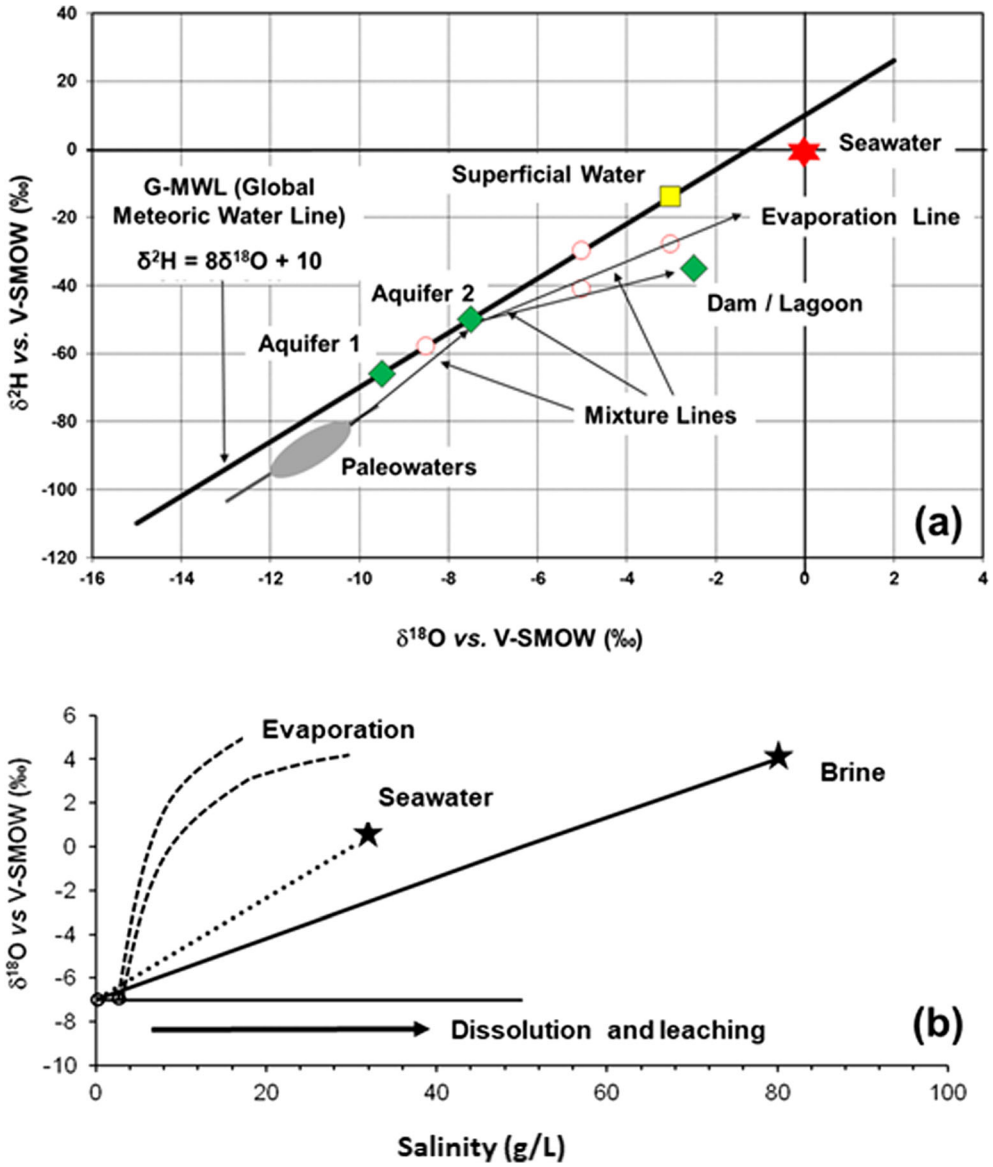

Fig. 3 **a** δ^2H vs. $\delta^{18}O$, showing the possible processes that may be able to modify the initial isotopic composition of the groundwater: examples of various mixing lines and hypothetical aquifers are represented. **b** Stable isotopic composition ($\delta^{18}O$) versus salinity, with identification of the different salinization processes (dissolution of salts; mixing with seawater; mixing with a brine; and evaporation—adapted from Gonfiantini and Araguás-Araguás 1988)

under a different climatic regime, i.e. paleowaters are involved.

The use of both stable isotopes and radiocarbon as a dating tool in groundwater systems permits the use of $\delta^{18}O$ and δ^2H data as an archive of ancient climates. The isotopic composition of groundwater is controlled in the first instance by the isotopic composition of rainfall in the recharge area. This in turn, may fluctuate due to several effects: (1) modification in the vapour source conditions, (2) degree of rainout of air masses, (3) a shift in the source of moisture, and (4) change in the isotopic composition of the global ocean (global climatic variations). All these factors are climate-controlled (Rozanski et al. 1992; Edmunds 2005).

In groundwater salinization studies, it is common to try to identify a relation between the isotopic and hydrogeochemical groundwater evolution along the flow paths (Fig. 3b)—i.e., in dissolution processes the stable isotope concentration of the water remains invariable, while the water salinity increase is noticed. A different trend is observed when seawater intrusion is occurring or has occurred, with a parallel isotopic and mineralization enrichment (Fig. 3). This unique characteristic enables the identification of the main processes based on isotopic and geochemical data (Araguás-Araguás and Gonfiantini 1989; Edmunds and Droubi 1998; Carreira et al. 2014).

Radioactive isotopes (^3H and ^{14}C)

Tritium can be used as a global transient tracer for studying dynamics of the hydrological cycle or as a qualitative tracer in the identification of active recharge and mixing between different hydrogeological units (Avrahamov et al. 2010; Carreira et al. 2010). Due to its half-life of 12.32 years (Lucas and

Unterweger 2000), in hydrogeological studies its application as a dating tool is rather limited, but it has been widely used in hydrology as an age indicator for young groundwater. The large quantity of ^{3}H release into the atmosphere during the early 1960s is nowadays decreasing to environmental levels prior to the thermonuclear tests. Nevertheless, ^{3}H concentration is very useful not only as an indicator of active recharge of the aquifer systems but also in the identification of mixing between aquifer systems (deep aquifers with tritium-free water, and shallow aquifers with tritium detectable).

Radiocarbon, with a half-life of 5,730 years, occurs in atmospheric CO_2, living biosphere and the hydrosphere after its production by cosmic radiation and it is partly associated with nuclear activities (anthropogenic origin). The ^{14}C concentration of carbon-containing materials is often given in percent modern carbon (pmC). The apparent age of groundwater was calculated using the carbon-14 concentration measured in the total dissolved inorganic carbon (TDIC), using the following equations (Gonfiantini and Zuppi 2003):

$$t = 8267 \ln \frac{Co}{C} \tag{2}$$

$$Co = 100\ (\delta TDIC - \delta R).\ \frac{\left(1 + \frac{2.3\ \varepsilon_{13}}{1000}\right)}{(\delta s - \delta R + \varepsilon_{13})} \tag{3}$$

where C is the measured ^{14}C activity of TDIC in the groundwater sample expressed in pmC, and C_o stands for "initial" ^{14}C activity of TDIC (also in pmC). ^{14}C activity of soil CO_2 has an assumed value of 100 pmC, while δ_{TDIC} stands for the measured ^{13}C concentration of TDIC, δ_R is the ^{13}C concentration of the carbonates fraction in the reservoir rock matrix, δ_S represents the ^{13}C concentration of soil CO_2, and ε is the ^{13}C enrichment factor associated with dissolution of soil CO_2 in the infiltrating water. For ^{14}C, the enrichment factor during CO_2 dissolution is assumed to be $2.3\varepsilon_{13}$; the number 8267 stands for the mean lifetime of ^{14}C in years. The value $\delta_S = -22 \pm 2$ ‰ was adopted for calculating the initial ^{14}C activity using Eq. (2). The value of $\delta_R = 0 \pm 1$ ‰ was adopted for soil and rock carbonates present in the system. To account for fractionation during dissolution of soil CO_2 in the infiltrating water, two values for ε_{13}, 9.0 ± 0.1 and 9.7 ± 0.1 ‰, were used, representing Holocene and glacial conditions, respectively, to account for the temperature dependence of ε_{13} (Mook et al. 1974).

Essaouira Basin (Morocco): results and discussion

Several hydrogeological research studies have been focused on the groundwater salinization within Essaouira sedimentary basin, partially focused on the identification of the main mechanisms responsible for groundwater degradation. Different approaches have been used in the treatment of the chemical and isotopic data such as mass balance simulation and principal component analysis (PCA): Hsissou et al. 1999; Bahir et al. 2000, 2008, 2017; Galego Fernandes et al. 2009; Ouhamdoucha et al. 2017. According to these studies, the groundwater degradation can be ascribed to mixing with seawater in the littoral areas, whereas in inland regions the apparent contribution of Tidzi diaper to the groundwater salinization cannot be ignored. From the 20 groundwater samples collected during this study from boreholes, dug wells and springs (distributed from the coastline towards the central part of the basin), 15 represent the Turonian formations (karst aquifer system), and the remaining five represent the Plio-Quaternary aquifer.

Hydrogeochemical approach: water–rock interaction

The hydrogeochemical results obtained for the Essaouira groundwater samples are reflecting different water–rock interaction processes present along the different flow paths. The depth of the wells—boreholes (B) and dug wells (W)— in the Turonian aquifer varies between 170 and 13.5 m, while in the Plio-Quaternary aquifer the depth varies between 45.0 and 12.5 m. Through the Durov diagram (Fig. 4), it is noticed that most of the water samples from both aquifer systems at Essaouira are Ca-Mg-Na-HCO_3-Cl type. From a hydrogeochemical point of view, no clear difference can be found between the Turonian and Plio-Quaternary water samples. Essentially, only the pH values—and the NO_3 concentrations, see Table S1 of the electronic supplementary material (ESM)—signify a clear difference between the groundwater samples from the shallow and deep aquifers.

A cluster of three samples from the Turonian aquifer (BT9, ST7 and ST12) can be identified (Fig. 4) based on the low concentrations of Na and K and the highest concentrations of SO_4 and TDS. This facies (Ca-Mg-SO_4) should likely be associated with evaporitic minerals dissolution (gypsum) that were identified within Essaouira basin. The possibility that this type of composition can be ascribed only to anthropogenic contamination by agriculture does not seem feasible. However, the accrual of SO_4 associated with agricultural activities (use of fertilizers or pesticides) is a possibility, but this hypothesis is not corroborated by the nitrate concentrations found in these samples (Table S1 of the ESM). There is no strong correlation between NO_3 and SO_4 ($r = 0.21$). However the hypothesis of a denitrification mechanism within the system should not be disregarded; the coefficient of correlation between NO_3 and Cl is $r = 0.57$, although the correlation between the SO_4 and Cl ($r = 0.19$) is negligible. Another hypothesis to be considered is the intermittent application of fertilizers and pesticides which can lead to contamination of the shallow groundwaters. During its path through the unsaturated

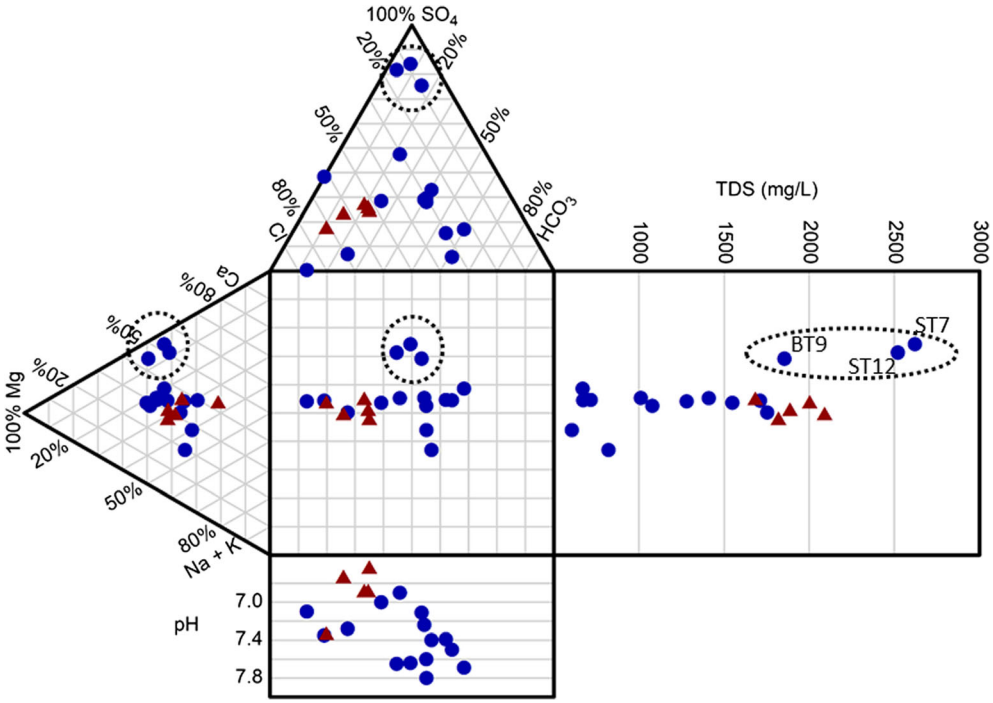

Fig. 4 Durov diagram for Essaouira basin: the brown triangles represent Plio-Quaternary groundwater samples and blue circles represent the Turonian groundwater samples. The cluster represented by dotted ellipses is probably due to gypsum dissolution

zone (soil), groundwater may gather anthropogenic contaminants from the regional application of fertilizers and pesticides, which could cause serious harm to the water resources. Consequently, some waters could be contaminated during their up-flow, from the groundwater reservoir to the ground surface, through processes of mixing with contaminated shallow groundwater (Ouhamdouch et al. 2015).

The anthropogenic influence in groundwater degradation is observed through nitrate determination, with concentrations varying from 0 up to 214 mg/L. The Plio-Quaternary water samples show the highest NO_3 concentration, with a mean around 99 ± 64.6 mg/L. A strong correlation between the NO_3 with Na and with Cl was found, respectively $r = 0.73$ and $r = 0.66$. Galego Fernandes et al. (2009) also mention the NO_3-Cl relation. Those authors associated this with an external origin for both ions with salt remobilization caused by precipitation after a long period of drought. The strong correlation (0.73) is possibly due to salts remobilization (increase of Cl, Na and NO_3) and simultaneously to more active anthropogenic influence in the basin. During water reuse by agriculture and any water up-flow, evaporation will induce a salt concentration increase. An additional NO_3 source could be attributed to the presence of the sodium nitrate mineral nitratine, although not mentioned in the lithological sequence of Essaouira basin. Nitratine can occur in semi-arid to arid environments. Nitrate can be replenished by occasional desert thunderstones, which fix N_2 from the air (webmineral.com 2016), supporting the NO_3 increase measured in the groundwater.

Minor correlation ($r = 0.1$ and $r = 0.2$ for the Turonian and Pliocene aquifers, respectively) is found between the pH values and the salinity, possibly indicating that the concentration of the dissolved salts is not related to the acid conditions of the groundwater but is mainly due to the dissolution of more soluble minerals (Manno et al. 2007), like gypsum and halite. Mass balance data were applied to identify the main mineral dissolution processes that could be responsible for the main geochemical features within the groundwater samples (Fig. 5).

Evaporate minerals dissolution was initially assumed to represent the main processes occurring in the groundwater flow paths from recharge area to discharge. In Fig. 5, evaporate minerals dissolution (1:1 straight lines) for calcite, dolomite, gypsum and halite are shown; however, none of the groundwater samples lies along the different trend lines. HCO_3 concentration is not strongly correlated either with Ca or with Mg concentration (Fig. 5a,b) pointing to a different origin, other than calcite or dolomite dissolution. This increase in Ca^{2+} and Mg^{2+} is detected in both aquifer systems in Essaouira basin. Highlighted in Fig. 5c, three water samples collected from the Turonian aquifer appear distant from the rest, and above the gypsum dissolution line, indicating an important income of sulphate, probably partly from gypsum dissolution and possibly also some contribution from anthropogenic activities (agriculture). Moreover, the Na^+ and Cl^- dissolved in the groundwater do not seem to be primarily associated with halite dissolution, and neither to seawater/freshwater mixing processes (Fig. 5d).

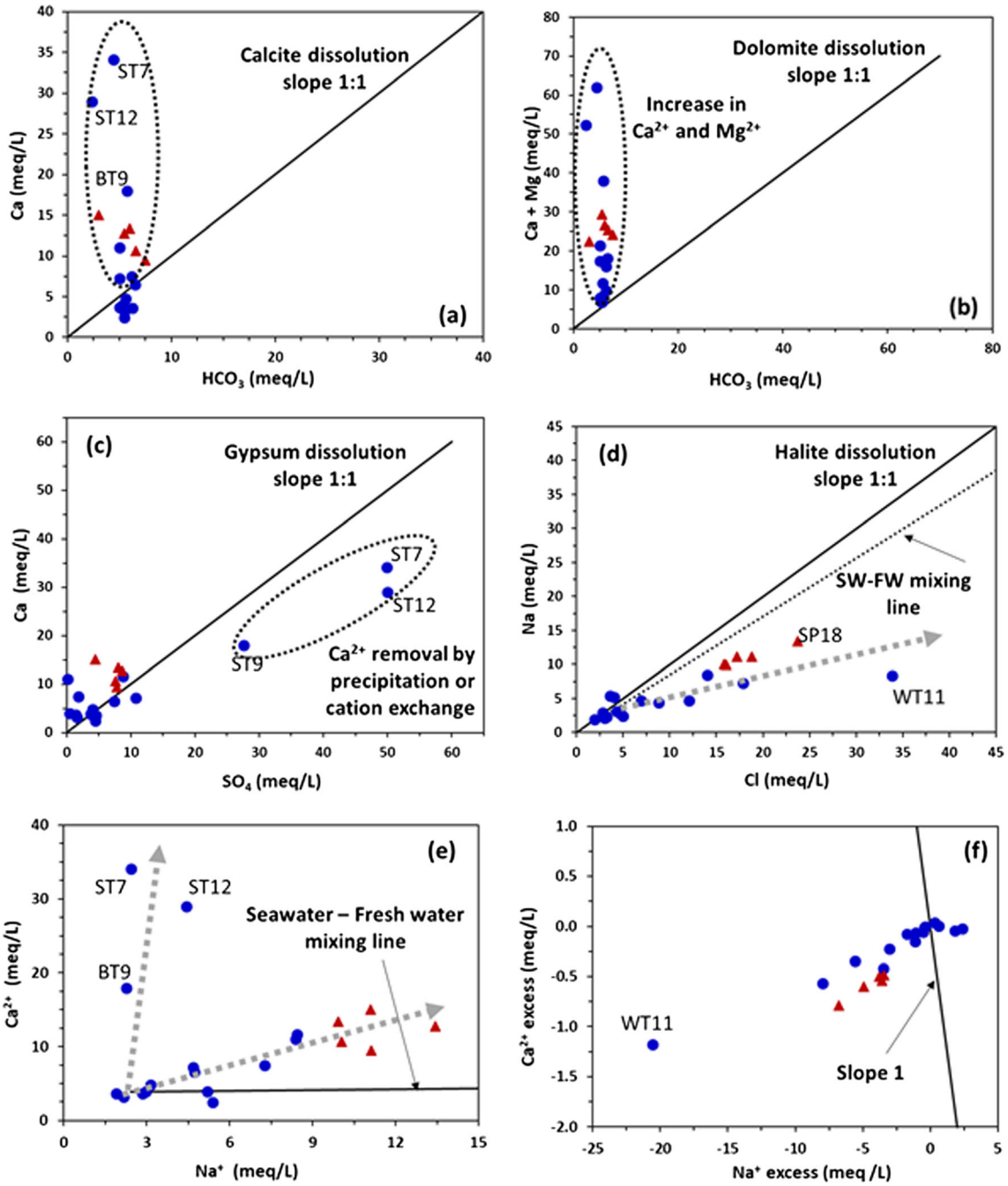

Fig. 5 Water–rock interaction in Essaouira groundwater samples, between different solutes: **a** Ca^{2+} vs. HCO_3^-; **b** Ca^{2+} + Mg^{2+} vs. HCO_3^-; **c** Ca^{2+} vs. SO_4^{2-}; **d** Na^+ vs. Cl^-; **e** Ca^{2+} vs. Na^+; **f** Ca^{2+}_{excess} vs. Na^+_{excess}, standing for ($\Delta n_{Ca} > 0$) and ($\Delta n_{Na} > 0$) respectively. The brown triangles represent Plio-Quaternary and blue circles represent the Turonian groundwater samples

Ionic exchange processes in different proportions are able to modify the ion concentration in the aqueous system. Several studies (Cates et al. 1996; Martínez and Bocanegra 2002; Pennisi et al. 2006; Carreira et al. 2014) point to the importance of subsurface adsorption of Na^+ by the aquifer matrix, with release of Ca^{2+}. According to those studies, this mechanism can be induced by intruded seawater in the geological formations. In order to estimate the importance of this process, ion exchange for Ca^{2+} and Na^+ was calculated by comparing the difference (Δn) of the measured concentration ($n_{(m)}$) and that expected if mixing with seawater is occurring ($n_{(c)}$). This Eq. (1) proposed by Pennisi et al. (2006) is based on the Cl^- concentration (conservative ion) and the "mobility behaviour" of Na and Ca.

In the Essaouira case study, these values represent the average composition of the groundwater samples with an electrical conductivity lower than 1,000 μS/cm (ST4; WT6 and BT10). Most of groundwater samples show Na^+ deficit ($\Delta n_{Na} < 0$) and none show Ca^{2+} excess ($\Delta n_{Ca} > 0$), which does not support the

hypothesis formulated that the missing Na^+ in the groundwater could be the result of cation exchange processes (Fig. 5e,f). Additionally, the saturation indexes (Table 1) of the evaporate minerals show that all water samples are saturated with respect to calcite and dolomite (except for BT1, SP18 and SP19) but under-saturated with respect to gypsum and halite, with the exception of samples ST7 and ST12. The variability in both salinity and ion composition found in the groundwater samples, points to a lithological heterogeneity in the region, which may change considerably from one part of the basin to another.

Isotopic approach - Essaouira basin

The $\delta^{18}O$ and $\delta^{2}H$ composition of Essaouira groundwater samples plot along the global meteoric water line (GMWL), and along the local meteoric water line (LMWL) presented by Rachid et al. (2014), roughly parallel to the GMWL (Fig. 6a). The groundwater samples indicate a meteoric origin, not significantly affected by evaporation. The Plio-Quaternary aquifer (mean composition) shows an enriched isotopic composition when compared with the Turonian water samples, around 0.7 ‰ in oxygen-18 and around 6‰ in deuterium (Table 1). The different isotopic concentrations found between the two aquifers are due to the different recharge altitudes. The main recharge area of the Plio-Quaternary aquifer is located on the Essaouira plain, while recharge of the Turonian aquifer probably takes place in the High Atlas Mountains (the highest peak range, elevation of 4,167 m above sea level (a.s.l.). The isotopic depletion measured in sample WP16 could be associated with mixing with the Turonian aquifer; this hypothesis is also supported by the Plio-Quaternary average value of 23 °C.

Plotting the oxygen-18 concentration as function of the total dissolved solids (TDS), Cl^-, Na^+ and SO_4^{2-} concentration (Fig. 6b–e), no clear trend in the seawater/freshwater characteristics is found. The samples with the highest mineralization are dispersed, not clearly indicating a mixing mechanism, neither a dissolution process. Only three groundwater samples from the Turonian aquifer appear as outliers due to SO_4 enrichment, which could be associated with gypsum dissolution or to anthropogenic activities (Fig. 6e).

Tritium concentration was determined in 10 water samples with concentrations varying between 0 and 3.4 TU, indicating an active recharge of the aquifer systems (Table 1). In contrast, the carbon-14 determinations carried out in five wells do not agree with the tritium presence in the groundwater system (samples BT1, WT5 and SP18). As mentioned in the preceding, the apparent radiocarbon age of groundwater was calculated using the carbon-14 concentration measured in the TDIC in the present groundwater (Eqs. 2 and 3). The apparent carbon-14 ages obtained vary from modern to 2.78 ka.

Table 1 Saturation indexes and isotopic data of the groundwater samples from Essaouira research area

Sample Ref.	SI_{Cal}	SI_{Dol}	SI_{Gyps}	SI_{Hal}	$\delta^{18}O$ (‰)	$\delta^{2}H$ (‰)	^{3}H (TU)	^{14}C (pmC)	$\delta^{13}C$ (‰)	Apparent age (ka)
BT1	−0.178	−0.234	−0.772	−6.213	−5.39	−31.4	1.3	67.4	−10.44	1.59
BT2	0.355	0.780	−1.503	−5.610	−4.71	−26.6	0.4	–	–	–
WT3	0.096	0.323	−1.262	−6.560	−5.43	−31.4	1.9	–	–	–
ST4	0.277	0.371	−2.162	−6.745	−5.69	−32.7	3.4	–	–	–
WT5	0.137	0.444	−1.749	−6.857	−5.68	−33.3	1.7	60.5	−10.82	2.78
WT6	0.455	0.974	−1.722	−7.115	−5.32	−31.6	2.0	–	–	–
ST7	0.903	1.622	0.200	−6.706	−5.43	−34.3	0.4	–	–	–
WT8	0.355	0.897	−1.330	−6.566	−5.59	−34.2	–	–	–	–
BT9	0.376	0.764	−0.156	−6.898	−5.88	−35.7	–	86.0	−5.12	Modern
BT10	0.603	1.276	−1.331	−6.375	−5.29	−29.1	0.2	–	–	–
WT11	0.215	0.430	−2.455	−5.288	−5.63	−35.1	1.0	–	–	–
ST12	0.693	1.297	0.225	−6.216	−5.48	−34.3	–	–	–	–
BT13	0.048	0.377	−1.410	−6.415	−5.25	−29.8	–	–	–	–
BT14	0.070	0.437	−0.947	−5.978	−4.90	−28.9	–	–	–	–
WT15	ND	ND	ND	−6.213	−3.82	−20.7	–	–	–	–
WP16	0.205	0.462	−0.688	ND	−6.21	−38.4	–	60.0	−7.41	Modern
WP17	0.100	0.355	−0.833	−5.555	−4.70	−24.5	–	–	–	–
SP18	−0.084	−0.051	−0.750	−5.546	−4.81	−27.6	0.8	74.4	−8.45	Modern
SP19	−0.144	−0.067	−0.668	−5.255	−4.90	−27.9	–	67.7	−9.18	Modern
WP20	0.369	0.443	−0.875	−5.477	−4.20	−23.7	–	–	–	–

Note: *B* borehole, *W* dug well, and *S* spring; *T*Turonian formations (deep), *P* Plio-Quaternary layers (shallow), SI_{Cal} calcite saturation index, SI_{Dol} dolomite saturation index, SI_{Gyps} gypsum saturation index, SI_{Hal} halite saturation index, *ND* not determined

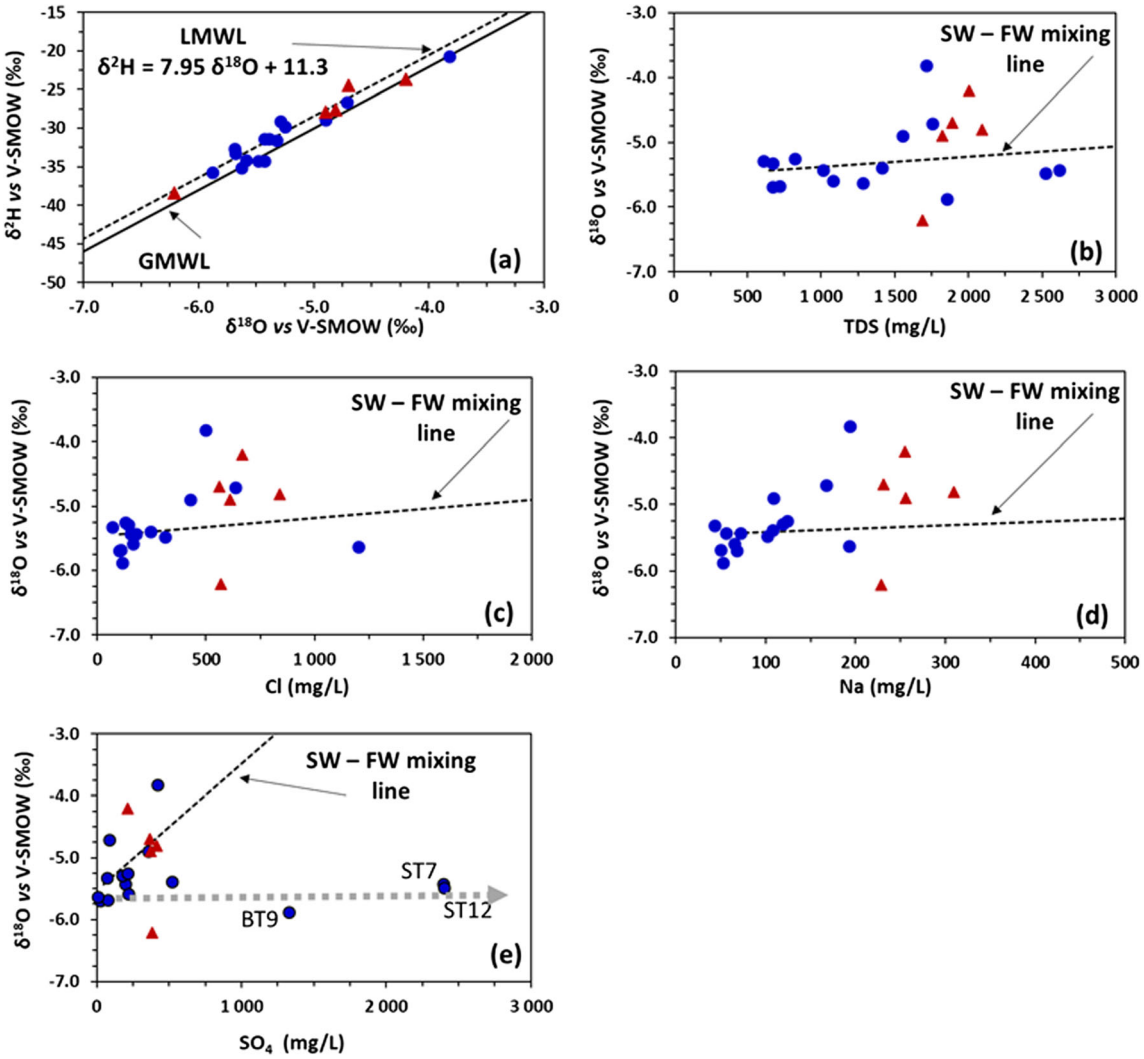

Fig. 6 Essaouira basin: **a** δ^2H vs. $\delta^{18}O$; **b** $\delta^{18}O$ vs. TDS; **c** $\delta^{18}O$ vs. Cl^-; **d** $\delta^{18}O$ vs. Na^+; **e** $\delta^{18}O$ vs. SO_4^{2-}. SW–FW seawater–freshwater; LMWL local meteoric water line (Rachid et al. 2014). The freshwater mean composition (end member) was calculated using the mean values of the groundwater samples that have electrical conductivity lower than 1,000 µS/cm; ($\delta^2H = -31.1$ ‰; $\delta^{18}O = -5.43$ ‰; TDS = 650.7 mg/L; Cl = 104.03 mg/L; Na = 55.75 mg/L; SO_4 = 45.75 mg/L). The brown triangles represent Plio-Quaternary and blue circles represent the Turonian groundwater samples

The presence of tritium in "old" groundwater samples BT1 and WT5 can be associated with the contribution of 'dead' carbon from the dissolution of carbonate minerals to the groundwater system, meaning that the groundwater samples are much younger than the obtained apparent ages (Table 1). This hypothesis is supported by the groundwater alkalinity values higher than 300 mg/L as wells as a high NO_3^- concentration, indicating most probably anthropogenic influence.

Lower Tagus–Lower Sado basin (Portugal): results and discussion

The Lower Tagus–Lower Sado aquifer system represents an important water resource for a large region that is highly populated and industrialized. Over the last few decades, this aquifer system has been extensively exploited, leading to an increase in the groundwater mineralization and to a growing concern regarding the quality of the water for human supply, agriculture and industry. From the recharge area towards the coastline, an increase in the groundwater mineralization is observed. The salt concentration (TDS) varies from 80 mg/L near the recharge area, up to around 8,000 mg/L near the coastline (Fig. 2). However, this mineralization tendency is disrupted by the Pinhal Novo graben; geophysical studies performed by Astier (1979) in the region indicate the presence of a "saline formation" connected to the Pinhal Novo graben structure that allows mineralisation to rise.

Several hydrogeological studies have been conducted in the region using hydrodynamic, hydrogeochemical, geophysics and environmental isotope approaches to investigate the main sources of salinization in the groundwater system

(Simões 2003; Carreira et al. 1994, 2014). These studies showed that the mineralization should be ascribed to uncontrolled exploitation, inducing: (1) mixing with highly polluted shallow aquifers; (2) active seawater intrusion and/or (3) salinization ascribed to brine dissolution detected at depth by geophysical studies. Ancient seawater trapped in the sediments, a brine formation unit or a diapiric structure at depth are possible structures that can be responsible for the groundwater salinization increase.

Hydrogeochemical approach: water–rock interaction

Natural processes of water–rock interaction are the main mechanisms responsible for water mineralization along the Sado basin, although this trend can be locally disturbed by anthropogenic action in agricultural areas, by the application of fertilizers or even due to the salts concentration by evaporation of irrigation water (Simões 1998, 2003). Analysing the physical and chemical results obtained for the groundwater samples collected in the different fieldwork campaigns, a progressive increase in the TDS is observed. The salts concentration varies from 80 up to 2,565 mg/L in the shallow Pliocene, while in the deeper Miocene aquifer it reaches values between 200 and 8,000 mg/L near Sado River (Table S2 of the ESM). In the discharge zones, the rise of the more mineralized waters, occasionally thermal waters (~26 °C), is detected. These mineralized waters can be partly related with mixing with ancient seawater trapped in the sediments or with brine dissolution mechanisms. Additionally, the tectonic structures found in the basin can act as preferential pathways of this deep groundwater to the surface. A gradual change from Ca-HCO_3 type waters to a Na-Cl type is observed when the groundwater-sample composition is plotted on a Durov diagram (Fig. 7).

The Pliocene and Mio-Pliocene water samples have distinctly lower pH values when compared with the Miocene; two evolutionary trends can be recognized based on the anion concentrations, one associated with an increase in the Cl^- concentration, the other established by SO_4^{2-} enrichment. An evolutionary pattern towards the seawater composition identified in the TDS distribution suggests that mixing between seawater and freshwater is occurring in the Miocene aquifer.

The lack of correlation ($r = 0.21$) between the groundwater mineralization (TDS) and the pH indicates that dissolved salts concentration in the water is related to the dissolution of most soluble minerals present in the aquifer matrix and not to the more-or-less acid environment (Manno et al. 2007). In order to find out the significance of the dissolution process within the groundwater evolution, Ca^{2+}, Mg^{2+} and Na^+ concentrations were plotted versus HCO_3^-, SO_4^{2-} and Cl^- (Fig. 8).

Two trend lines are observed (Fig. 8a,b), related to Ca and Mg, pointing to different sources other than calcite and/or dolomite dissolution. Ca enrichment is also noticed when plotted vs. SO_4 concentration (Fig. 8c). A group of samples

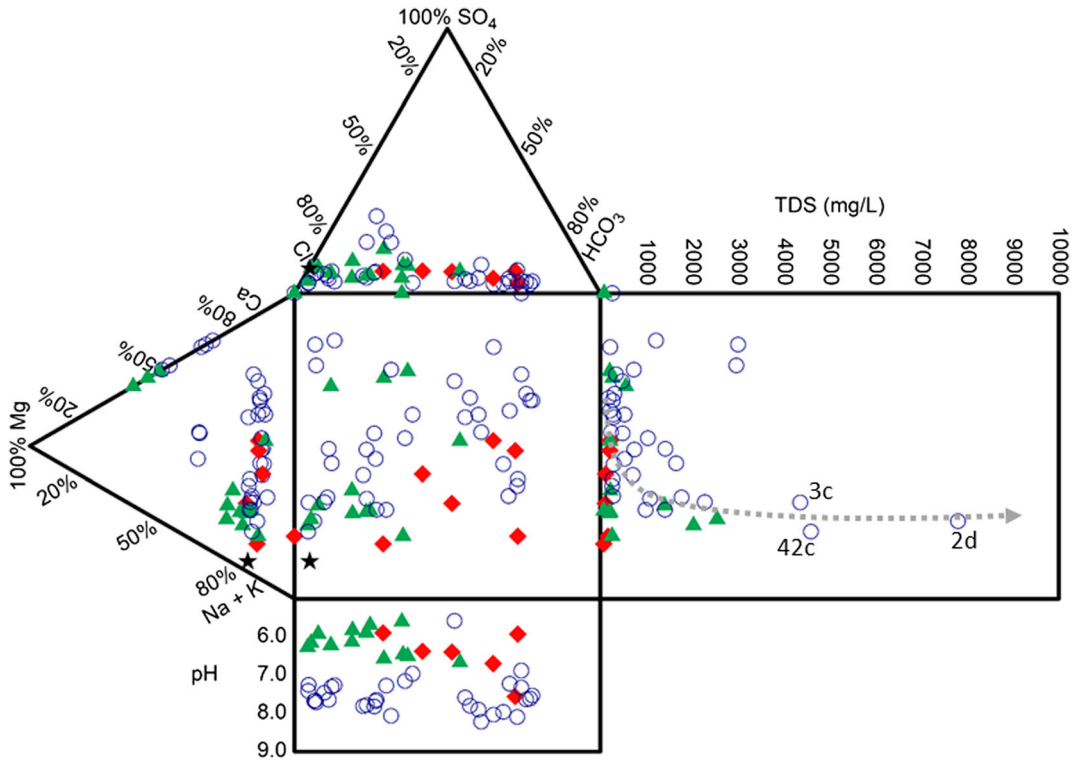

Fig. 7 Durov diagram for Lower Tagus-Lower Sado basin: The green triangles represent Pliocene; the red diamond represent the Mio-Pliocene and blue circles represent the Miocene groundwater samples. The stars represent the mean seawater composition

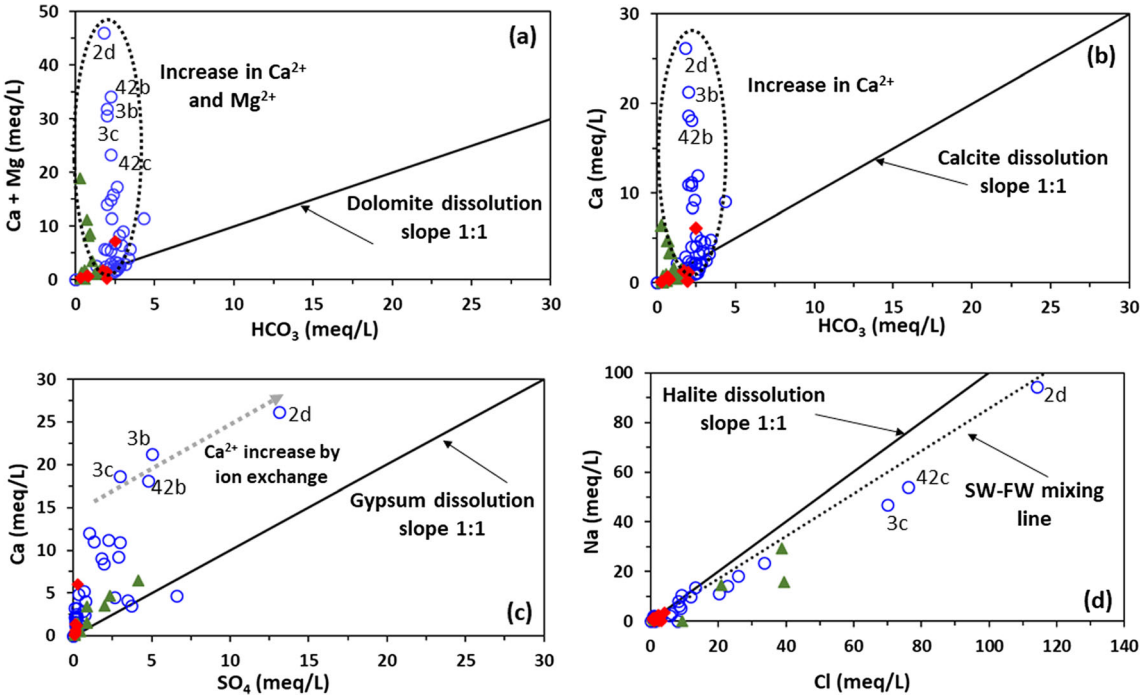

Fig. 8 Water–rock interaction between different solutes for Lower Tagus–Lower Sado groundwater samples: **a** Ca^{2+} + Mg^{2+} vs. HCO_3^-; **b** Ca^{2+} vs. HCO_3^-; **c** Ca^{2+} vs. SO_4^{2-} and **d** Na^+ vs. Cl^-. The green triangles represent Pliocene; the red diamonds represent the Mio-Pliocene and blue circles represent the Miocene groundwater samples

appears isolated, more enriched in Ca, possibly due to ion exchange mechanisms and higher contribution of gypsum dissolution; these samples define a parallel trend line to the 1:1 gypsum dissolution line.

A strong correlation between the Na and the Cl concentration ($r = 0.98$) is obtained for the groundwater samples. When represented in an orthogonal diagram, the samples are placed along the seawater/freshwater mixing line, approximately close to the halite dissolution line (Fig. 8d), indicating an important mechanism responsible for the groundwater geochemical signatures. Yet, another process must be investigated to clarify the depletion in Na. The Na^+ decrease could be associated with ion exchange mechanisms, corroborating not only the Na decrease but also the Ca enrichment (Fig. 8c,d). To verify this hypothesis, the mean composition of the groundwater symbolising the "initial composition (freshwater component)" was calculated assuming the average electrical conductivity was lower than 1,000 μS/cm ($n = 20$).

The increase in the groundwater mineralization is consistent with an increase in the saturation indexes, as observed in samples from the Miocene aquifer (Fig. 9). Some of the samples are saturated with respect to calcite and dolomite, but all are under-saturated with respect to gypsum. When the Ca^{2+} and Mg^{2+} concentrations are plotted versus HCO_3^- concentration, the samples do not locate near the calcite or dolomite dissolution lines (1:1 line). This inconsistency could be due to ion exchange mechanisms along the groundwater flow path, explaining the two different evolution trends in the Ca^{2+} and Na^+ plot, both above the line of seawater/freshwater mixing (Fig. 9e); this reflects the lithological heterogeneities inside the sedimentary basin, and ionic exchange mechanisms, with different proportions. The Eq. (1) proposed by Pennisi et al. (2006) was applied (Fig. 9e,f); most groundwater samples present a Na^+ deficit ($\Delta n_{Na} < 0$) and an excess of Ca^{2+} ($\Delta n_{Ca} > 0$), corroborating the hypothesis that the missing Na^+ and increasing Ca^{2+} concentration is ascribed to ion exchange mechanisms.

Isotopic approach: Lower Tagus–Lower Sado Basin

Most of the groundwater samples collected in the Lower Tagus–Lower Sado basin are distributed along the GMWL, although a different trend is defined by the seven groundwater samples from the Miocene aquifer. These seven samples draw a parallel line to the GMWL (Table 2); thus, there is no strong evidence of evaporation prior to infiltration (Fig. 10). One possible explanation for this isotopic deviation is that the recharge occurred under a different climatic regime—a colder period (Carreira et al. 2014) towards the last glacial maximum (LGM).

The isotopic composition of the glacial ocean is not well defined; however, the available information estimates of changes in $\delta^{18}O$ range from +1.3‰ (Fairbanks and Matthews 1978) to +1.0 ‰ (Schrag et al. 2002). During the LGM the European continent remained under prevailing westerly circulation, with an isotopic continental effect for both

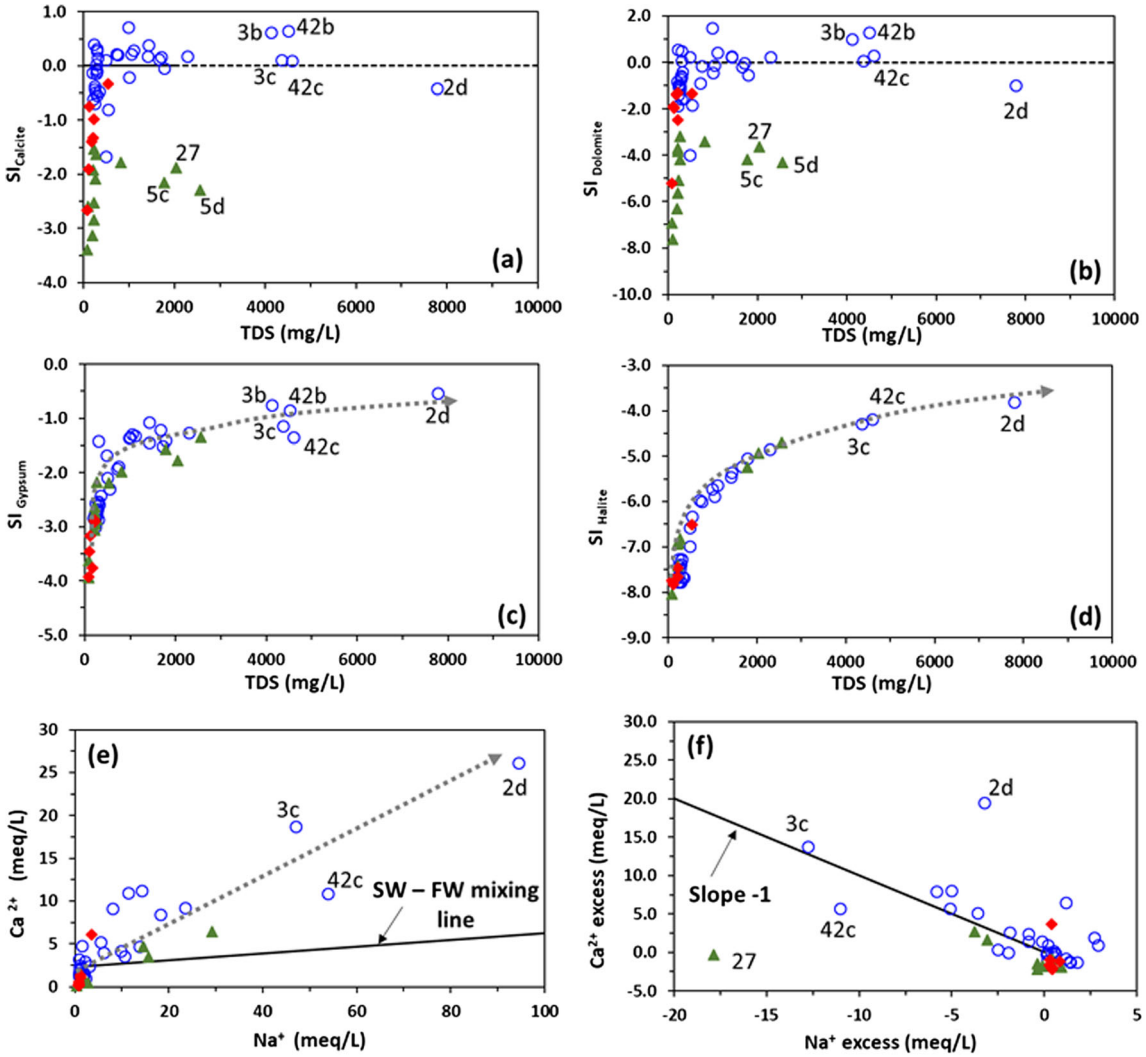

Fig. 9 Water–rock interaction, dissolution processes for Lower Tagus–Lower Sado groundwater samples: **a** $SI_{Calcite}$ vs. TDS; **b** $SI_{Dolomite}$ vs. TDS; **c** SI_{Gypsum} vs. TDS; **d** SI_{Halite} vs. TDS; **e** Ca vs. Na; **f** $Ca^{2+}{}_{excess}$ vs. $Na^{+}{}_{excess}$. The green triangles represent Pliocene; the red diamonds represent the Mio-Pliocene and blue circles represent the Miocene groundwater samples. Part **f** of the figure is adapted from Carreira et al. 2014

δ^2H and $\delta^{18}O$, similar to the present-day value. (Rozanski 1985; Schrag et al. 2002). The Lower Tagus–Lower Sado system is located on the Atlantic Coast, it would receive precipitation mainly from a first-step condensation of maritime moist air masses. Thus, the isotopic fluctuations of the source (ocean) will have visible impact on the isotopic composition of the newly formed groundwater, greater than the global temperature decrease.

When the ^{18}O isotopic composition of the groundwater samples is plotted versus the TDS, Cl^-, Na^+ or SO_4^{2-} concentrations, the samples with the highest mineralization plot over or very close to the seawater/freshwater mixing line (Fig. 10), suggesting that this process is mainly responsible for the groundwater salinization. This hypothesis is corroborated by ionic exchange mechanisms in different proportions along the flow paths that can be triggered when seawater intrusion is occurring.

The tritium determinations were carried out on all the groundwater samples collected during the four fieldwork campaigns. In the Pliocene aquifer samples, the tritium (^3H) concentration varies between 1 and 3 TU (Table 2), yet no tritium was found in the Miocene groundwater samples. Radiocarbon determinations carried out on the TDIC varied in the Pliocene samples from 71.9 ± 0.7 to 88 ± 0.8 pmC, and from 2.9 ± 0.3 up to 45.6 ± 0.9 pmC in the Miocene groundwater samples.

The apparent radiocarbon age of the groundwater samples was calculated using Eqs. (2) and (3). A simple model was used, since the saturation index with respect to calcite is not significant, and the $\delta^{13}C$ concentration in the TDIC of the groundwater samples is around −10 ‰, indicating a minor contribution recognised as carbonate dissolution. The estimated apparent carbon-14 ages of the groundwater samples vary between modern (Pliocene aquifer samples 5 and 27) up to

Table 2 Isotopic composition and apparent carbon-14 age of the Lower Tagus–Lower Sado groundwater samples

Sample Ref.	TDS (mg/L)	δ^2H (‰)	$\delta^{18}O$ (‰)	^3H (TU)	$\delta^{13}C$ (‰)	$^{14}C \pm$ (pmC)	^{14}C apparent age (ka)
1 (M)	1,425	−23.6	−4.29	–	–	–	–
2 (M)	749	–	−4.18	–	–	–	–
2a (M)	1,199	−22.6	−4.23	1.4	–	–	–
2b (M)	1,708	−27.8	−4.3	–	–	–	–
2c (M)	1,660	−25.4	−4.29	–	−10.4	12.9 ± 0.9	14.6 ± 2.8
2d (M)	7,783	−17.8	−3.48	–	–	–	–
3 (M)	1,781	–	−4.09	–	–	–	–
3a (M)	3,395	−26.1	−4.01	–	−9.2	8.4 ± 0.8	17.2 ± 3.0
3b (M)	4,121	−25.7	−4.16	–	–	–	–
3c (M)	4,364	−23.0	−4.44	1.4	−7.3	6.7 ± 0.6	17.1 ± 3.1
3d (M)	298	−21.7	−4.48	–	−10.0	2.9 ± 0.3	26.6 ± 3.1
4 (M)	539	−28.0	−4.73	1.3	−12.1	5.9 ± 0.5	22.3 ± 2.9
5 (P)	226	–	−4.58	–	–	–	–
5a (P)	642	−25.6	−4.63	0.3	–	–	–
5b (P)	817	−29.7	−4.68	–	–	–	–
5c (P)	1,775	−29.3	−4.68	–	−17.9	88.1 ± 0.8	3.2 ± 2.5
5d (P)	2,558	−20.6	−4.3	1.4	–	–	–
6 (M)	238	−31.4	−4.81	–	–	–	–
7 (M)	713	−23.6	−4.23	–	–	–	–
8 (M)	298	–	−4.27	–	–	–	–
8a (M)	–	−23.3	−4.24	–	–	–	–
8b (M)	219	−26.7	−4.51	0.8	–	–	–
8c (M)	291	−21.6	−4.37	–	–	–	–
9 (M-P)	216	−24.3	−4.52	–	–	–	–
10 (M-P)	113	−23.8	−4.73	–	–	–	–
11 (M)	261	−24.2	−4.36	–	–	–	–
12 (M-P)	82	−23.2	−4.65	1.2	–	–	–
13 (M-P)	124	−24.4	−4.58	–	–	–	–
14 (M-P)	175	−23.4	−4.63	–	–	–	–
15 (P)	81	−25.8	−4.75	–	–	–	–
16 (M-P)	219	−25.0	−4.58	–	–	–	–
17 (M)	266	−25.7	−4.71	1.4	–	–	–
18 (P)	113	−24.8	−4.61	1.6	–	–	–
19 (P)	90	−21.1	−4.56	–	–	–	–
21 (P)	218	−28.2	−5.05	2.6	−17.6	71.9 ± 0.7	4.8 ± 2.5
22 (P)	261	−24.8	−4.75	–	–	–	–
23 (P)	272	−27.3	−4.57	–	–	–	–
24 (P)	213	−28.2	−4.67	–	–	–	–
25 (M)	314	−26.7	−4.50	–	–	–	–
26 (P)	198	−26.3	−4.74	–	–	–	–
27 (P)	2,043	−24.5	−4.50	–	−10.0	85.6 ± 3.3	Modern
28 (M)	348	−27.0	−4.59	–	–	–	–
29 (P)	219	−27.3	−4.75	–	–	–	–
30 (M)	214	−24.6	−4.64	–	–	–	–
31 (M)	1,043	−23.6	−4.34	–	−10.5	45.8 ± 0.6	4.2 ± 2.6
32 (M-P)	535	−27.6	−4.65	–	−12.9	32.8 ± 0.5	8.7 ± 2.5
33 (M)	296	−22.5	−4.60	–	–	–	–
34 (M)	481	−24.0	−4.57	–	–	–	–
35 (M)	191	−22.2	−4.64	–	–	–	–
36 (M)	280	−22.9	−4.62	–	–	–	–
37 (M)	274	−24.6	−4.35	–	–	–	–
38 (M)	1,415	−26.1	−4.61	–	–	–	–
39 (M)	490	−25.8	−4.58	–	−10	10.8 ± 0.7	15.8 ± 2.8
42 (M)	2,287	–	−4.09	–	–	–	–
42a (M)	3,929	−20.9	−3.17	–	−8.1	5.6 ± 1.2	19.5 ± 4.4
42b (M)	4,507	−24.2	−3.88	–	–	–	–
42c (M)	4,594	−21.4	−3.88	–	–	7.1 ± 1.2	17.4 ± 3.9
43 (M)	810	–	−4.41	–	–	–	–
43a (M)	875	−23.6	−4.37	–	−6.95	3.1 ± 0.4	23.1 ± 3.5
43b (M)	979	−29.1	−4.59	1	–	–	–
43c (M)	994	−27.9	−4.65	–	−7.08	4.0 ± 0.4	21.1 ± 3.2

Note: *P* Pliocene aquifer; *M-P* Mio-Pliocene aquifer, *M* Miocene aquifer

26.6 ± 3.1 ka BP (Miocene aquifer sample 3d). The ^{14}C apparent ages obtained for the deepest aquifer indicate the possible presence of paleowaters (with exception of borehole 31), with an average age around 19 ka BP (Table 2), pointing to a possible recharge during the LGM.

Two evolution trend lines for the Miocene groundwater samples can be identified when the groundwater mineralization (TDS or Cl^- concentration) is plotted against the apparent groundwater age, possibly established by different salt origins: brine dissolution, evaporitic dome dissolution, or ancient seawater trapped in the sediments. Equally, active seawater intrusion appears to play the dominant role in water mineralization of the Pliocene aquifer in the northern part of the basin, near the Tagus River, where the increase of salinization is not followed by a groundwater age increase (Fig. 10f). The strong positive correlation between mineralization and ageing of the groundwater indicates mixing with ancient seawater trapped in the sediments of the basin during its formation. This trapped seawater has no ^{14}C in their composition, and thus is ^{14}C free. In this case, the increase of salts in the groundwater system may be ascribed to the ancient seawater trapped in the sediments during the sedimentary basin formation. A similar effect was presented by Sukhija et al. (1996) for a coastal area of Madras, India, and by Avrahamov et al. (2010) in a research project carried out on the saline groundwater in the Dead Sea area (Middle East) involving attempts to date brines. Those projects distinguished paleomarine and modern seawater intrusion on the basis of a combined approach using radiocarbon, tritium and hydrogeochemical data.

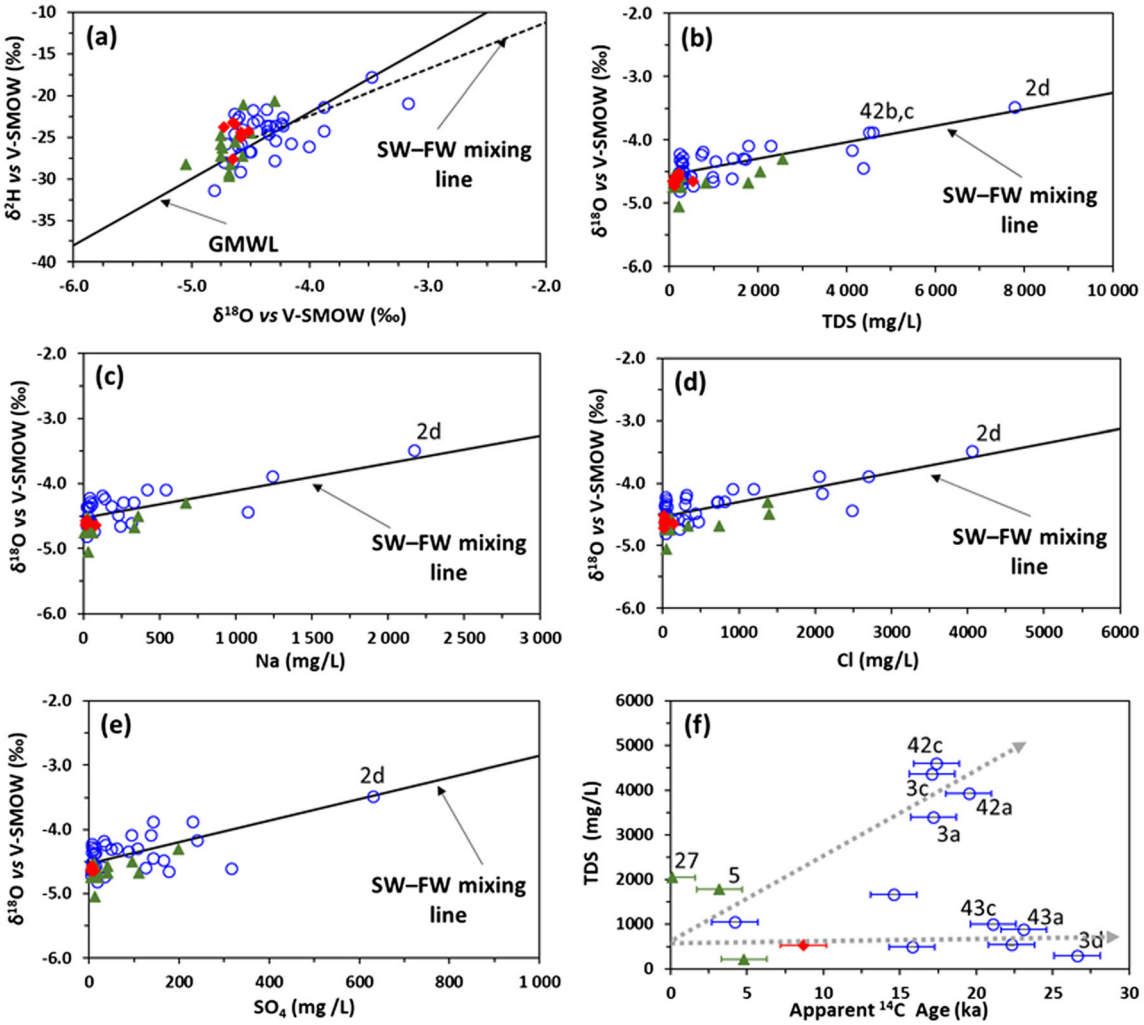

Fig. 10 Lower Tagus–Lower Sado basin: **a** δ^2H vs. $\delta^{18}O$; **b** $\delta^{18}O$ vs. TDS; **c** $\delta^{18}O$ vs. Na^+; **d** $\delta^{18}O$ vs. Cl^-; **e** $\delta^{18}O$ vs. SO_4^{2-} and **f** TDS vs. Apparent ^{14}C age. The green triangles represent Pliocene; the red diamonds represent the Mio-Pliocene and blue circles represent the Miocene groundwater samples. Part **b** of the figure adapted from Carreira et al. 2014. SW–FW seawater–freshwater

Assuming that recharge of the deep aquifer took place during the LGM, the relation between the ^{14}C apparent groundwater ages of samples and their isotopic composition (δ^2H and $\delta^{18}O$) was investigated in order to identify the "presence of a cooler period" recorded in the groundwater system. The research works carried out by the authors on Aveiro coastal aquifer, northern Portugal (Carreira et al. 1996; Carreira 1998), found a different isotopic evolution from the European continent, i.e. the paleowaters infiltrated during the LGM are more enriched than the modern regional precipitation. This pattern was also observed in Namibia and in the Florida coastal aquifers, USA (Vogel et al. 1982; Plummer 1993). One possible explanation for this difference in trend must be related to the preferential removal of the lighter isotopic species (^1H and ^{16}O) during polar ice cap formation. This isotopic fractionation induced an isotopic enrichment in the residual oceanic water. According to the results of the aforementioned projects in Aveiro, Namibia, and Florida, coastal-aquifer isotopic composition will reflect (1) the isotopic modifications that occurred in the ocean during that period, and not the atmospheric temperature variations, and (2) the position of the polar front during the LGM. Great Britain and all of Central Europe were covered by an ice mass, while the Iberian Peninsula (the Sado Basin and Aveiro) experienced a colder climate of about 5–6 °C, values supported by noble gases determinations (Carreira 1998; Edmunds 2005).

In the case of the Lower Tagus–Lower Sado basin, the groundwater dating indicates the presence of paleowaters recharged during the LGM; however, the isotopic indicator of a different colder period for this time period will be masked by the mixing with a different water body (ancient seawater mixing). Nevertheless, the mean isotopic composition was estimated using the isotopic composition data of all water samples with a TDS < 650 mg/L from the deep (Miocene) aquifer (maximum limit of salinity settled to calculate the mean isotopic composition of the groundwater) in the region,

and the mean isotopic composition of the shallow aquifer (Pliocene). The difference in ^{18}O content for these two aquifers is 0.20 ‰ (Miocene aquifer: $\delta^{18}O_{mean} = -4.54 \pm 0.14$ ‰, $n = 17$; Pliocene aquifer: $\delta^{18}O_{mean} = -4.71 \pm 0.15$ ‰, $n = 9$). The Miocene aquifer is isotopically enriched when compared with Plio-Miocene or Pliocene waters. This may indicate an isotopic composition evolution similar to the one observed in Aveiro palaeowaters (Carreira et al. 1996).

Final remarks

Coastal groundwater resources represent relatively multifaceted systems that are not easy to understand, are under complex hydrogeological conditions and often involve human intervention. In previous research, this type of system was studied in a "simple way", where seawater intrusion was the only mechanism considered able to modify the groundwater composition. Knowledge is sought on the origins of the salinity and the means of preventing the salinity impacts, and therefore the use of integrated geochemical and isotopic methods is important to understand the wide range of salinity issues. This knowledge is fundamental in the context of deterioration of water quality resulting from anthropogenic actions such as pollution or over abstraction of groundwater resources. Among the human factors, the intensification of salinity directly by pollution or indirectly by agricultural activities, and/or excessive pumping, will lead to intrusion of saline groundwater into the freshwater system. Environmental isotopes together with the geochemical data provide, beyond question, an effective marker for seawater and freshwater, and enable tracing of seawater intrusion and identification of processes that may be responsible for water salinization.

Comparison synopsis: Essaouira vs. Sado basin

The main goal of this work was to understand the salinization processes present in the groundwater systems of two sedimentary basins under similar climate and geological settings, using comparable approaches. In Essaouira basin, the groundwater salinity does not increase linearly down gradient; no clear trend of seawater/freshwater mixing was identified by the geochemical approach or by use of isotopes. The groundwater samples from the shallow Miocene aquifer are dispersed and did not clearly point to a mixing mechanism or to dissolution processes, as the major processes responsible for the mineralization increase. However, the water samples from the shallow aquifer are strongly correlated by TDS and Cl^-, indicating that chemical reactions within the aquifer are clearly occurring through halite dissolution. Active recharge is occurring and, based on tritium concentration and by using the ^{18}O fractionation with altitude, one can assume that the recharge area for the deep aquifer should be in the High Atlas Mountains, about 200 km from Essaouira. The apparent carbon-14 ages obtained vary from modern to 2.78 ka BP. The discrepancy between ^{3}H and ^{14}C concentrations in the water–rock interaction processes must call on the contribution of 'dead' carbon from the carbonate minerals to the groundwater system, leading to older carbon-14 apparent ages (Table 1). This hypothesis is supported by the groundwater composition with alkalinity values higher than 300 mg/L as well as a high NO_3^- concentration, indicating most probably anthropogenic influence and partially to dissolution of the sodium nitrate mineral nitratine. No paleoclimatic record was identified within the Essaouira basin's deep groundwater system.

In contrast, in the Lower Tagus–Lower Sado basin, the natural processes of water–rock interaction are the main mechanisms responsible for water mineralization, although intermittent evidence of anthropogenic activity in some agricultural areas is found (salt concentrations increase in the groundwater by evaporation of the irrigation water and via the impact of fertilizer usage). Two different geochemical evolution trends, both diverging from the seawater/freshwater mixing line, are associated with different flow paths with different percentages of carbonate minerals. Ion exchange mechanisms occurring along the groundwater flow path are able to influence the ion concentration of the water, especially Ca^{2+} and Na^+. The groundwater geochemical characteristics and distribution within the basin are influenced by the occurrence of a heterogeneous saltwater/freshwater interface, due to the layering of the coastal aquifer system, and the interface moves inland. The alternative hypothesis—that of carbonate-equilibrium control of the alkaline earth elements and proportional Na increase associated with dissolution of evaporitic minerals—seems not be applicable in this particular case.

The apparent groundwater age estimated for the deeper Miocene aquifer (average value) is around 19 ka BP, indicating the presence of paleowaters. Active seawater intrusion appears to play a major role in the groundwater mineralization in the shallow Pliocene aquifer, in the northern part of the basin; the increasing trend in salt concentration is not followed by groundwater ageing. However, in the southern area of the basin, near Setúbal, the deeper groundwater salinization is linked to an increase of the apparent ^{14}C ages. In this case, the increase of salts in the groundwater system can be ascribed to ancient seawater trapped in the sediments, during the sedimentary basin formation. Besides this, the isotopic enrichment observed in the Miocene aquifer when compared with the Pliocene water samples, was most probably caused by isotopically heavier ocean water during the last glacial maximum (LGM).

Conclusions

The use of geochemicals and isotopes as tracers to identify and characterize the origin of salts in groundwater systems

proved to be more effective when used simultaneously. In the two case studies (in Morocco and Portugal), the joint use of geochemical and isotopic tracers (stable and radioactive environmental isotopes) proved to be highly effective in the identification of salinization origin. The groundwater stable isotopic composition (δ^2H or $\delta^{18}O$) demonstrated, without any doubt, to be a unique tool to distinguish between seawater mixing and dissolution of evaporitic minerals (halite). Complementary groundwater dating using ^{14}C helped to distinguish between the modern or ancient saltwater bodies that are mixing with the freshwater system such as seawater, brackish or brine waters. This joint approach provided a better understanding of the variable nature of groundwater mineralization, which can help to optimize the use of groundwater resources in coastal regions.

Acknowledgements An early draft of this manuscript was critically read by two anonymous reviewers and the authors gratefully acknowledge their contribution. Ayden George Sellwood is thanked for editing the English language text.

Funding information These studies were funded by International Atomic Energy Agency – Isotope Hydrology Section. The C^2TN/IST authors acknowledge the Foundation for Science and Technology (FCT) support through the UID/Multi/04349/2013 project.

References

Araguás-Araguás L, Gonfiantini R (1989) Environmental isotopes in sea water intrusion studies. International Atomic Energy Agency, Internal Report, IAEA, Vienna

Astier JL (1979) Etude des resources en eaux souterraines de la péninsule de Setúbal – Portugal. Geophysique. Nouveaux résultats de la prospection électrique [Study of the groundwater resources of the peninsula of Setúbal - Portugal: geophysics—new results of electrical prospecting]. UNDP–UNESCO, Paris

Avrahamov N, Yechieli Y, Lazar B, Lewenberg O, Boaretto E, Sivan O (2010) Characterization and dating of saline groundwater in the Dead Sea area. Radiocarbon 52(2–3):1123–1140

Bahir M, Mennani A, Jalal M, Youbi N (2000) Contribution à l'étude des ressources hydriques du bassin synclinal d'Essaouira (Maroc) [Contribution to the study of water resources of Essaouira synclinal basin (Morocco)]. Estud Geol 56:185–195

Bahir M, Carreira P, Oliveira da Silva M, Fernandes P (2008) Caractérisation hydrodynamique, hydrochimique et isotopique du système aquifère de Kourimat (Bassin d'Essaouira, Maroc) [Hydrodynamic, hydrochemical and isotopic characterization of the Kourimat aquifer system (Essaouira Basin, Morocco)]. Estud Geol 64(1):61–73

Bahir M, El Moukhayar R, Carreira P, Souhel A (2015) Isotopic tools for groundwater management in semi-arid area: case of the Wadi Ouazzi Basin (Morocco). Larhyss J 23:23–39

Bahir M, Carreira PM, Ouhamdouchc S, Chamchati H (2017) Recharge conceptual model and mineralization of groundwater in a semi-arid region; Essaouira basin (Morocco). Procedia Earth Planet Sci 17: 69–72. https://doi.org/10.1016/j.proeps.2016.12.036

Ben Hamouda MF, Carreira P, Marques JM, Eggenkamp HGM (2013) Geochemical and isotopic investigations to study the origin of mineralization of the coastal aquifer of Sousse. Tunisia Proc Earth Planet Sci 7:61–64. https://doi.org/10.1016/j.proeps.2013.03.063

Bouchaou L, Michelot JL, Vengosh A, Hsissou Y, Qurtobi M, Gaye CB, Bullen TD, Zuppi GM (2008) Application of multiple isotopic and geochemical tracers for investigation of recharge, salinization, and residence time of water in the Souss–Massa aquifer, southwest of Morocco. J Hydrol 352:267–287. https://doi.org/10.1016/j.jhydrol.2008.01.022

Bouzourra H, Bouhlila R, Elango L, Slama F, Ouslati N (2015) Characterization of mechanisms and processes of groundwater salinization in irrigated coastal area using statistics, GIS, and hydrogeochemical investigations. Environ Sci Pollut Res 22:2643–2660. https://doi.org/10.1007/s11356-014-3428-0

Broughton P, Trepanier A (1993) Hydrocarbon generation in the Essaouira basin of western Morocco. Bull Am Assoc Petrol Geol 77:999–1015

Carreira PM (1998) Paleoáguas de Aveiro [Aveiro palaeowaters]. PhD Thesis, Aveiro University, Aveiro, Portugal

Carreira PM, Macedo ME, Soares AMM, Vieira MC, Santos JB (1994) Origem da salinização do sistema aquífero da Bacia do Baixo Sado, na região de Setúbal [Origin of salinization of the aquifer system of the Lower Sado Basin, in Setubal region]. Recursos Hídricos 15(1): 41–48

Carreira PM, Soares AMM, Silva MAM, Araguás-Araguás L, Rozanski K (1996) Application of environmental isotope methods in assessing groundwater dynamics of an intensively exploited coastal aquifer in Portugal. In: Isotopes in water resources management, vol 2. IAEA, Vienna, pp 45–58

Carreira PM, Marques JM, Pina A, Mota Gomes A, Galego Fernandes P, Monteiro Santos FA (2010) Groundwater assessment at Santiago Island (Cabo Verde): a multidisciplinary approach to a recurring source of water supply. Water Resour Manag 24:1139–1159. https://doi.org/10.1007/s11269-009-9489-z

Carreira PM, Marques JM, Nunes D (2014) Source of groundwater salinity in coastline aquifers based on environmental isotopes (Portugal): natural vs. human interference—a review and reinterpretation. Appl Geochem 41:163–175. https://doi.org/10.1016/j.apgeochem.2013.12.012

Carvalho MR, Almeida C (1989) HIDSPEC, um programa de especiação e cálculo de equilíbrios água/rocha. [HIDSPEC, a program of speciation and calculation of water / rock balances]. Rev. Univ. Aveiro 4 (2), 1–22

Cates DA, Knox RC, Sabatini DA (1996) The impact of ion exchange processes on subsurface brine transport as observed on Piper diagrams. Ground Water 34(3):532–544

Coplen TB, De Bièvre P, Krouse HR, Vocke RDJr, Groening M, Rozanski K (1996) Ratios for light-element isotopes standardized for better interlaboratory comparison, Eos, v. 77 (27): 255pp. https://doi.org/10.1029/96EO00182

Custodio E (2002) Aquifer overexploitation: what does it mean? Hydrogeol J 10(2):254–277. https://doi.org/10.1007/s10040-002-0188-6

Custodio E (2010) Coastal aquifers of Europe: an overview. Hydrogeol J 18(1):269–280. https://doi.org/10.1007/s10040-009-0496-1

Edmunds WM (2005) Groundwater as an archive of climatic and environmental change. In: Aggarwal PK, Gat JR, Froehlich KFO (eds) Isotopes in the water cycle: past, present and future of a developing science. Springer, The Netherlands, pp 341–352

Edmunds WM, Droubi A (1998) Groundwater salinity and environmental change. In: Isotopetechniques in the study of environmental change. IAEA, Vienna, pp 503–518

Epstein S, Mayeda T (1953) Variation of 18O content of waters from natural sources. Geochim. Cosmochim. Acta 4: 213–224

Fairbanks RG, Matthews RK (1978) The marine oxygen isotope record in Pleistocene coral, Barbados. West Indies Quatern Res 10:181–196

Foster S, MacDonald A (2014) The 'water security' dialogue: why it needs to be better informed about groundwater. Hydrogeol J 22: 1489–1492. https://doi.org/10.1007/s10040-014-1157-6

Friedman I (1953) Deuterium content of natural waters and other substances. Geochim. Cosmochim. Acta 4: 89–103

Galego Fernandes P, Carreira PM (2008) Isotopic evidence of aquifer recharge during the last ice age in Portugal. J Hydrol 361:291–308. https://doi.org/10.1016/j.jhydrol.2008.07.046

Galego Fernandes P, Carreira PM, Bahir M (2009) Mass balance simulation and principal components analysis applied to groundwater resources: Essaouira basin (Morocco). Environ Earth Sci 59(7):1475–1484. https://doi.org/10.1007/s12665-009-0133-2

Gonfiantini R, Araguás-Araguás LA (1988) Los isotopos ambientales en los estudios de la intrusion marina [The environmental isotopes in marine intrusion studies]. Proc. Symp. Tecnológia de la Intrusión en acuíferos Costeros, Ponencias Internacionales, 1. IGME, Madrid, pp 135–190

Gonfiantini R, Zuppi GM (2003) Carbon isotopic exchange rate of DIC in karst groundwater. Chem Geol 197:319–336. https://doi.org/10.1016/S0009-2541(02)00402-3

Hsissou Y, Mudry J, Mania J, Bouchaou L, Chauve P (1999) Utilisation du rapport Br/Cl pour déterminer l'origine de la salinisation des eaux souterraines: exemple de la Plaine du sous (Maroc) [Use of the Br/Cl ratio to determine the origin of salinization of groundwater: example of the plain of sous (Morocco)]. Comptes Rendus de l'Académie des sciences - series IIA. Earth Planet Sci 328(6):381–386. https://doi.org/10.1016/S1251-8050(99)80103-7

IAEA (1976) Procedure and technique critique for tritium enrichment by electrolysis at IAEA Laboratory. Technical Procedure n°19. International Atomic Energy Agency, Vienna

IAEA (2014) Groundwater Sampling Procedures for Isotope Hydrology. International Atomic Energy Agency. Water Resources Programme http://www-naweb.iaea.org/napc/ih/documents/other/2014%20ENG%20Gw%20Sampling%20booklet%20-%20separate%20pages.pdf. Accessed 27 June 2018

Jalali M (2007) Salinization of groundwater in arid and semi-arid zones: an example from Tajarak, western Iran. Environ Geol 52:1133–1149. https://doi.org/10.1007/s00254-006-0551-3

Kim Y, Lee KS, Koh DC, Lee DH, Lee SG, Park WB, Koh GW, Woo NC (2003) Hydrogeochemical and isotopic evidence of groundwater salinization in a coastal aquifer: a case study in Jeju volcanic island. Korea J Hydrol 270:282–294

Langman JB, Ellis AS (2010) A multi-isotope (δD, $\delta^{18}O$, $^{87}Sr/^{86}Sr$, and $\delta^{11}B$) approach for identifying saltwater intrusion and resolving groundwater evolution along the western Caprock escarpment of the southern High Plains, New Mexico. Appl Geochem 25:159–174. https://doi.org/10.1016/j.apgeochem.2009.11.004

Lucas LL, Unterweger MP (2000) Comprehensive review and critical evaluation of the half-life of tritium. J Res Natl Inst Technol 105: 541–549

Manno E, Vassallo M, Varrica D, Dongarrà G, Hauser S (2007) Hydrogeochemistry and water balance in the coastal wetland area of "Biviere di Gela" Sicily, Italy. Water Air Soil Pollut 178:179–193. https://doi.org/10.1007/s11270-006-9189-8

Martínez DE, Bocanegra EM (2002) Hydrogeochemistry and cation-exchange processes in the coastal aquifer of Mar Del Plata, Argentina. Hydrogeol J 10:393–408. https://doi.org/10.1007/s10040-002-0195-7

Medina F (1989) Landsat imagery interpretation of Essaouira basin (Morocco): comparison with geophysical data and structural implications. J Afr Earth Sci 9 (1): 69–75

Mondal NC, Singh VS, Saxena VK, Singh VP (2011) Assessment of seawater impact using major hydrochemical ions: a case study from Sadras, Tamilnadu, India. Environ Monit Assess 177:315–335. https://doi.org/10.1007/s10661-010-1636-8

Mook WG, Bommerson JC, Staverman WH (1974) Carbon isotope fractionation between dissolved bicarbonate and gaseous carbon dioxide. Earth Planet Sci Lett 22:169–176

Ouhamdouch S, Bahir M, Chkir N, Carreira P, Goumih A (2015) Comportement hydrogeochimique d'un aquifere cotier des zones semi-arides: cas de l'aquifere Barremien-Aptien du bassin d'Essaouira (Maroc occidental) [Hydrogeochemical behavior of a coastal aquifer in semi-arid zones: case of the Barremian-Aptian aquifer of the Essaouira basin (western Morocco)]. Larhyss J 25:163–182

Ouhamdoucha S, Bahir M, Carreira PM (2017) Geochemical and isotopic tools to deciphering the origin of mineralization of the coastal aquifer of Essaouira basin, Morocco. Procedia Earth Planet Sci 17:73–76. https://doi.org/10.1016/j.proeps.2016.12.038

Pennisi M, Bianchini G, Muti A, Kloppmann W, Gonfiantini R (2006) Behaviour of boron and strontium isotopes in groundwater–aquifer interactions in Cornia plain (Tuscany, Italy). Appl Geochem 21: 1169–1183. https://doi.org/10.1016/j.apgeochem.2006.03.001

Plummer LN (1993) Stable isotope enrichment in paleowaters of the Southeast Atlantic coastal plain, US. Science 262:2016–2020

Pulido-Leboeuf P (2004) Seawater intrusion and associated processes in a small coastal complex aquifer (C astell de Ferro, Spain). Appl Geochem 19:1517–1527

Rachid EM, Bahir M, Chamchati H, Najiba C, Carreira PM, Naserrddin Y (2014) Using geochemical and isotope investigations for groundwater management strategies under semi-arid area: case of the Wadi Ouazzi basin (Morocco). J Environ Earth Sci 4(7):18–30

Re V, Zuppi GM (2011) Influence of precipitation and deep saline groundwater on the hydrological systems of Mediterranean coastal plains: a general overview. Hydrol Sci J 56:966–980. https://doi.org/10.1080/02626667.2011.597355

Re V, Sacchi E, Martin-Bordes JL, Aureli A, El Hamouti N, Bouchnan R, Zuppi GM (2013) Processes affecting groundwater quality in arid zones: the case of the Bou-Areg coastal aquifer (North Morocco). Appl Geochem 34:181–198. https://doi.org/10.1016/j.apgeochem.2013.03.011

Rozanski K (1985) Deuterium and oxygen-18 in European groundwaters: links to atmospheric circulation in the past. Chem Geol (Isotope Geosci Sec) 52:349–363

Rozanski K, Araguás-Araguás L, Gonfiantini R (1992) Relation between long-term of oxygen-18 isotope composition of precipitation and climate. Science 258:981–985

Schrag DP, Adkins JF, McIntyre K, Alexander JL, Hodell DA, Charles CD, McManus JF (2002) The oxygen isotopic composition of seawater during the last glacial maximum. Quatern Sci Rev 21:331–342

Shi JA, Wang Q, Chen GJ, Wang GY, Zhang ZN (2001) Isotopic geochemistry of the groundwater system in arid and semiarid areas and its significance: a case study in Shiyang River basin, Gansu province, Northwest China. Environ Geol 40(4–5):557–565. https://doi.org/10.1007/s002540000196

Simões MMM (1998) Contribuição para o conhecimento hidrogeológico do cenozoico na Bacia do Baixo Tejo [Contribution to the hydrogeological knowledge of the Cenozoic in the Lower Tagus Basin]. PhD Thesis, Universidade Nova de Lisboa, Portugal

Simões M (2003) On the hydrogeology of the Lower Tagus Basin and its Cenozoic geologic evolution. Ciências Terra 15:239–248

Stadler S, Sültenfu J, Holländer HM, Bohn A, Jahnke C, Suckow A (2012) Isotopic and geochemical indicators for groundwater flow and multi-component mixing near disturbed salt anticlines. Chem

Geol (294–295):226–242. https://doi.org/10.1016/j.chemgeo.2011.12.006

Sukhija BS, Varma VN, Nagabhushanam P, Reddy DV (1996) Differentiation of palaeomarine and modern seawater intruded salinities in coastal groundwaters (of Karaikal and Tanjavur, India) based on inorganic chemistry, organic biomarker fingerprints and radiocarbon dating. J Hydrol 174:173–201

Vogel JC, Talma AS, Heaton THE (1982) The age and isotopic composition of groundwater in the Stampriet artesian Basin, SWA National Physical Research Laboratory. Council of Scientific and Industrial Research, Pretoria, South Africa

webmineral.com (2016) Nitratine mineral data. http://webmineral.com/data/Nitratine.shtml#.VrHsa_mLSUk. Accessed December 2016

Werner AD (2010) A review of seawater intrusion and its management in Australia. Hydrogeol J 18(1):281–285. https://doi.org/10.1007/s10040-009-0465-8